Tree height uncertainty biases aboveground biomass estimation more than wood density in miombo woodlands

Arthur M. Yambayamba[1,2*], Ferdinand Handavu[3], Kondwani Kapinga[4,5], Tommaso Jucker[1]

Affiliations

[1]School of Biological Sciences, University of Bristol, Bristol, UK

[2]School of Natural Resources, Copperbelt University, Kitwe, Zambia

[3]Department of Geography, Environment and Climate Change, Mukuba University, Kitwe, Zambia

[4]Dag Hammarskjöld Institute for Peace and Conflict Studies (DHIPS), Environment, Sustainable Development and Peace, Copperbelt University, Kitwe, Zambia

[5]Chair of Environment and Development, Oliver R. Tambo Africa Research Chair Initiative (ORTARChI), Copperbelt University, P.O. Box 21692, Kitwe, Zambia

Corresponding author

Arthur M. Yambayamba, School of Biological Sciences, University of Bristol, 24 Tyndall Avenue, Bristol, BS8 1TQ, UK.

Email: arthur.yambayamba@bristol.ac.uk or ympazi@gmail.com

17 **ABSTRACT**

18 Accurate and unbiased estimation of tree aboveground biomass (*AGB*) is essential for large-
19 scale monitoring of forest carbon stocks. But estimating *AGB* typically requires several data
20 imputation steps that can introduce substantial errors that are hard to quantify and correct for.
21 Two sources of uncertainty that are thought to be particularly important but remain
22 understudied are tree height – which is generally estimated using allometric models – and wood
23 density – which is most commonly assigned from databases based on taxonomic matching.
24 Here we used data from 155 destructively harvested trees in Zambia's miombo woodlands that
25 span a large range of sizes to quantify errors in *AGB* arising from uncertainty in tree height and
26 wood density. We found that when locally-calibrated height-diameter allometries are used to
27 estimate missing tree height information and when wood density is imputed from species-
28 specific values derived from public databases, *AGB* can be estimated with high precision and
29 little or no bias. However, when tree height and wood density are imputed more coarsely using
30 data that are not biome specific, errors in *AGB* can be substantial. Specifically, estimating tree
31 height using a regional allometric model developed for tropical dry forests led to
32 underestimating *AGB* by nearly 30%. Our study underscores the importance of accurately
33 accounting for tree height and wood density to estimate *AGB*, thereby paving the way for more
34 robust estimation of forest carbon stocks and their uncertainties across a range of ecosystem
35 types.

36 **Key words**: forest carbon; destructive sampling; allometry; power law scaling; Bayesian
37 regression

1. INTRODUCTION

Forests and savannas play a crucial role in regulating the terrestrial carbon cycle by sequestering large amounts of carbon dioxide (CO_2) from the atmosphere and storing it as woody biomass (Rathgeber et al., 2016). This potential of forests to act as long-term carbon sinks, that slow the pace of climate change by partially offsetting anthropogenic CO_2 emissions, has gained widespread attention in recent decades (Grantham et al., 2020; Ellis et al., 2021; Arias et al., 2021). This has led to growing interest in restoration programs centered around forest creation and expansion (Lewis et al., 2019; Hua et al., 2024), as well as burgeoning international forest carbon markets underpinned by programs such as REDD+ (Bomfim et al., 2022) and dedicated satellite missions to map global forest carbon stocks (Quegan et al., 2019; Dubayah et al., 2020). However, a fundamental assumption of these efforts is that forest carbon stocks can be estimated accurately and without bias. In practice, this is rarely the case even at the most basic level of the individual tree (Demol et al., 2024; Fareed and Numata, 2024; Terryn et al., 2024), as there are multiple sources of uncertainty that affect tree biomass estimation and we lack a clear understanding of their relative importance and magnitude.

A fundamental unit of forest carbon stock estimation is a tree's aboveground woody biomass (*AGB*). Direct measurements of *AGB* involves destructive sampling to weigh the trunk and branches, which in addition to killing the tree is laborious and costly (Clark and Kellner, 2012; Colgan et al., 2013). In practice, *AGB* is therefore almost always estimated using allometric equations that have been calibrated using data from relatively small numbers of trees whose mass has been destructively measured (Chave et al., 2004) – although more recently terrestrial laser scanning is being increasingly used to generate accurate, non-destructive estimates of tree woody volume and *AGB* (Momo Takoudjou et al., 2018; Calders et al., 2022; Demol et al., 2024). These allometric biomass equations typically rely on some combination of stem diameter at breast height (D), tree height (H), wood density (ρ) and, in rarer cases,

crown width as input variables (Chave et al., 2014; Goodman et al., 2014; Ploton et al., 2016; Jucker et al., 2017). A myriad of such equations exist (Henry et al., 2013; Chojnacky et al., 2014; Zianis et al., 2005), but among the most widely used for tropical trees is the pantropical model developed by Chave et al. (2014), which express *AGB* as a power-law function of $D^2 \times H \times \rho$ – a compound variable that approximates a tree's trunk volume ($D^2 \times H$) and multiplies this by the density of its wood to estimate *AGB*.

However, the estimation of *AGB* using such models can be greatly impacted by the quality of measurements or imputation of the input variables. In particular, while *D* is generally recorded accurately and precisely in forest inventories, the same is not true for *H* and ρ. Common approaches to measuring *H* in the field using clinometers and laser range finders are both difficult to do accurately and time consuming. When *H* is measured directly in the field, estimates are therefore often uncertain and in some cases systematically biased (Larjavaara and Muller-Landau, 2013; Sullivan et al., 2018; Terryn et al., 2024), with the height of tall trees often underestimated. More commonly, *H* is not measured at all, but is instead itself estimated from *D* using allometric equations (Fayolle et al., 2016; Sullivan et al., 2018). These *H–D* allometries not only propagate any underlying biases in the *H* measurements used to parameterize them, but can also introduce additional sources of uncertainty that are hard to quantify once scaled to *AGB*. This includes errors arising from the choice of functional form used to model *H–D* allometries (Fayolle et al., 2016; Ledo et al., 2016; Cano et al., 2019; Terryn et al., 2024) and the fact that *H–D* scaling relationships can vary considerably among tree species and forest types (Feldpausch et al., 2011; Banin et al., 2012; Jucker et al., 2022; Jucker et al., 2025).

Similarly, ρ is very rarely measured as part of field inventories and is instead almost always assigned from global databases based on taxonomic or geographic matching (Chave et al., 2009; Réjou-Méchain et al., 2017; Fischer et al., 2026). While these databases are

88 invaluable, they still only cover <15% of known tree species, meaning that in many cases ρ is
89 imputed using either taxonomic (e.g., genus or family-level means) or geographic proxies (e.g.,
90 plot or regional-level means). Depending on a region's taxonomic coverage in the database and
91 the choice of imputation method, uncertainty in ρ can therefore substantially bias *AGB*
92 estimates (Flores and Coomes, 2011; Mitchard et al., 2014; Phillips et al., 2019).

93 Here we provide a rigorous quantitative assessment of how uncertainty in both *H* and
94 ρ propagates to tree-level *AGB* estimates, focusing specifically on southern Africa's miombo
95 woodlands. Like other tropical dry forests, miombo woodlands remain underrepresented in the
96 research and conservation agenda despite being among the most extensive tropical dry forests
97 in Africa and globally (around 2 million km^2; (Ribeiro et al., 2020)) and storing substantial
98 amounts of carbon in their vegetation (around 20–30 Mg C ha^{-1}; (Mcnicol et al., 2018)). To
99 address this knowledge gap, we compiled data for 155 trees whose *AGB* was measured via
100 destructive sampling in the miombo woodlands of Zambia. These trees cover a wide spectrum
101 of sizes (D = 5.0–68.2 cm; H = 4.2–25.0 m) and represent 37 uniquely identified species that
102 vary considerably in their wood density (ρ = 0.34–0.86 g cm^{-3}). Using these data, we set out to
103 address three research objectives:

104 (1) Compare the predictive performance of existing local and pantropical biomass models
105 that differ in their functional form;
106 (2) Reparametrize existing biomass models with new data to assess how this improves
107 their fit;
108 (3) Determine how different approaches to imputing H and ρ affect tree-level *AGB*
109 estimates.

110

2. MATERIALS AND METHODS

2.1 Study system

The study was conducted using datasets acquired in miombo woodlands from three sites in the Copperbelt Province of Zambia – Mwekera, Miengwe and Katanino (Fig. 1). Miombo woodlands are characterized by the dominance of trees in the genus *Brachystegia* that form open-canopy habitats where trees and grasses co-exist. Regionally, they cover around 2 million km^2 of land, forming a belt that stretches from Angola's Atlantic coast to the Indian Ocean in Mozambique and Tanzania (Dziba et al., 2020). Miombo woodlands are shaped by long dry seasons (5–8 months), followed by months of intense rainfall which usually falls between November and April. Annual rainfall varies considerably across the region, from around 1600 mm in northern Zambia and southern DRC to as little as 600 mm in Angola and southern Zambia (Ribeiro et al., 2020). Accordingly, the woodlands can be divided into wet (>1000 mm) and dry miombo (<1000 mm), which differ in their structure and species composition (White, 1983). These woodlands are further shaped by human disturbances comprising mainly of fires, wood harvesting and land clearing for agriculture (Chidumayo, 2013a). Trees have evolved and adapted to these disturbances and recover remarkably quickly (Chidumayo, 2004; Syampungani et al., 2017), with aboveground carbon stocks returning to pre-disturbance levels in around 25–40 years (Williams et al., 2008; Mcnicol et al., 2015). However, regional aboveground carbon density estimates vary significantly among studies (15–72 Mg C ha^{-1} for mature woodlands; (Ribeiro et al., 2020)). While some of this variation reflects differences in climate, species composition and disturbance regimes (Handavu et al., 2021), it also arises from differences in the way *AGB* is estimated (Demol et al., 2024). This underscores the importance of resolving these sources of uncertainty to improve regional carbon stock estimates.

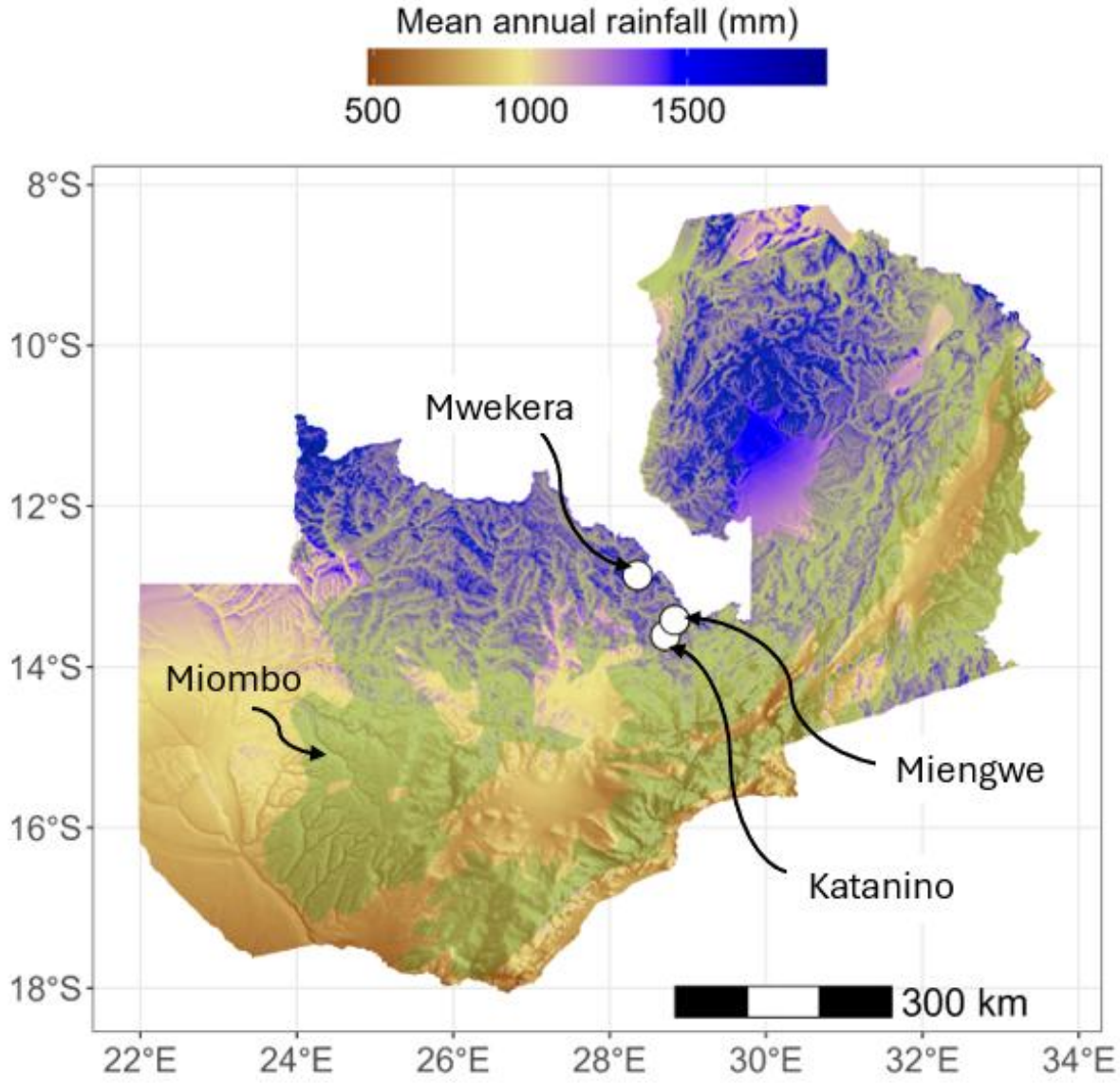


Figure 1. A map of Zambia showing the extent of the miombo woodlands (green shading) and the location of the three sites (white filled circles) from where the data used in the study were collected. The distribution of mean annual precipitation across the country shows the approximate locations of wet miombo (northern part) and dry miombo (southern part) within Zambia. Precipitation data was extracted from the CHELSA-BIOCLIM+ database at a spatial resolution of 30 arc-seconds (approximately 1 km) (Brun et al., 2022). The shapefile for miombo woodlands extent was obtained from Poppenwimer (2022) based on the description of ecoregions by Olson et al. (2001).

2.2 Tree harvest data

We compiled three separate datasets for which a combined total of 158 individual trees belonging to 37 tree species were destructively harvested to measure *AGB*. Prior to conducting destructive sampling, vegetation surveys were conducted to assign trees to different *D* classes (minimum *D* = 5 cm) from which a random subset was selected for harvesting. In all the three sites, *D* was measured to the nearest 0.1 cm using diameter tapes while *H* was measured using either a Suunto hypsometer (before trees were felled, at the Mwekera site) or a 50 m measuring tape (after felling trees at the other two sites). Selected trees were felled at ground level (<15 cm from the ground) and then cut into manageable segments of between 1–3 m using chain saws. The cut segments were then weighed for fresh mass in the field using the END-T3 weighing indicator with a capacity of 600 kg and a precision of 0.01 kg. Furthermore, all small branches, twigs and leaves were cut from each trunk and measured for mass (Kapinga et al., 2018; Handavu et al., 2021).

In addition to *AGB*, *D*, and *H*, the wood density (ρ, in g cm^{-3}) for each tree was also measured. Specifically, ρ was determined using sample discs cut from all wood components (trunk base, trunk segments, large and small branches) to account for variation in ρ within a tree. The cut discs were taken to the laboratory where they were oven dried at 105°C for 48 hours and then mass was determined using a scale with precision of 0.001 g. The oven dried discs were then submerged in water for 48 hours to reach saturation before determining the volume of green (fresh) wood. The volume for each disc was determined using the water displacement method using graduated cylinders. ρ was then calculated as the oven dry mass per unit volume of green wood (Kapinga et al., 2018; Handavu et al., 2021).

To rule out potential measurement errors that could unduly influence the calibration of *AGB* models, we used Cook's distance and studentized residuals to check for outliers in the bivariate relationship between *AGB* and *D* (on a log-log scale). Based on this, we identified

three data points that were flagged as outliers and excluded from further analysis (Fig. S1a). This left us with 155 trees for comparing and reparametrizing *AGB* models. This dataset covered a large spectrum of sizes (D = 5.0–68.2 cm; H = 4.2–25.0 m), with *AGB* ranging between 5.7–3209.9 kg and wood density ranging between 0.34–0.86 g cm^{-3} (Table 1 and see Fig. 2 for a summary of the tree harvest data and the relationship between *AGB* and its predictors).

Table 1. Breakdown of the tree harvest dataset for the three sites in miombo woodlands, including number of trees harvested and species, as well as the median and range (in square brackets) of stem diameter at breast height, total tree height, wood density, aboveground biomass, elevation, mean total annual precipitation and mean annual temperature.

	Katanino forest	**Miengwe forest**	**Mwekera forest**	**Combined dataset**
Number of trees harvested	12	94	49	155
Number of species	9	33	5	37
Stem diameter (D; cm)	22.6	21.3	22.0	21.4
	[12.2 – 46.0]	[5.0 – 52.2]	[5.5 – 68.2]	[5.0 – 68.2]
Tree height (H; m)	13.5	12.9	17.0	13.8
	[5.7 – 22.8]	[4.2 – 20.7]	[5.0 – 25.0]	[4.2 – 25.0]
Wood density (ρ; g cm^{-3})	0.64	0.60	0.64	0.61
	[0.49 – 0.86]	[0.42 – 0.82]	[0.34 – 0.85]	[0.34 – 0.86]
Aboveground biomass (*AGB*; kg)	301.0	217.7	230.6	219.2
	[27.2 - 2149.3]	[7.8 - 2374.4]	[5.7 – 3209.9]	[5.7 – 3209.9]
Mean elevation (m a.s.l.)	1323	1324	1228	[1228 – 1324]
Mean annual precipitation (mm yr^{-1})	1325	1250	1198	[1198 – 1325]
Mean annual temperature (°C)	20.1	20.2	20.9	[20.1 – 20.9]

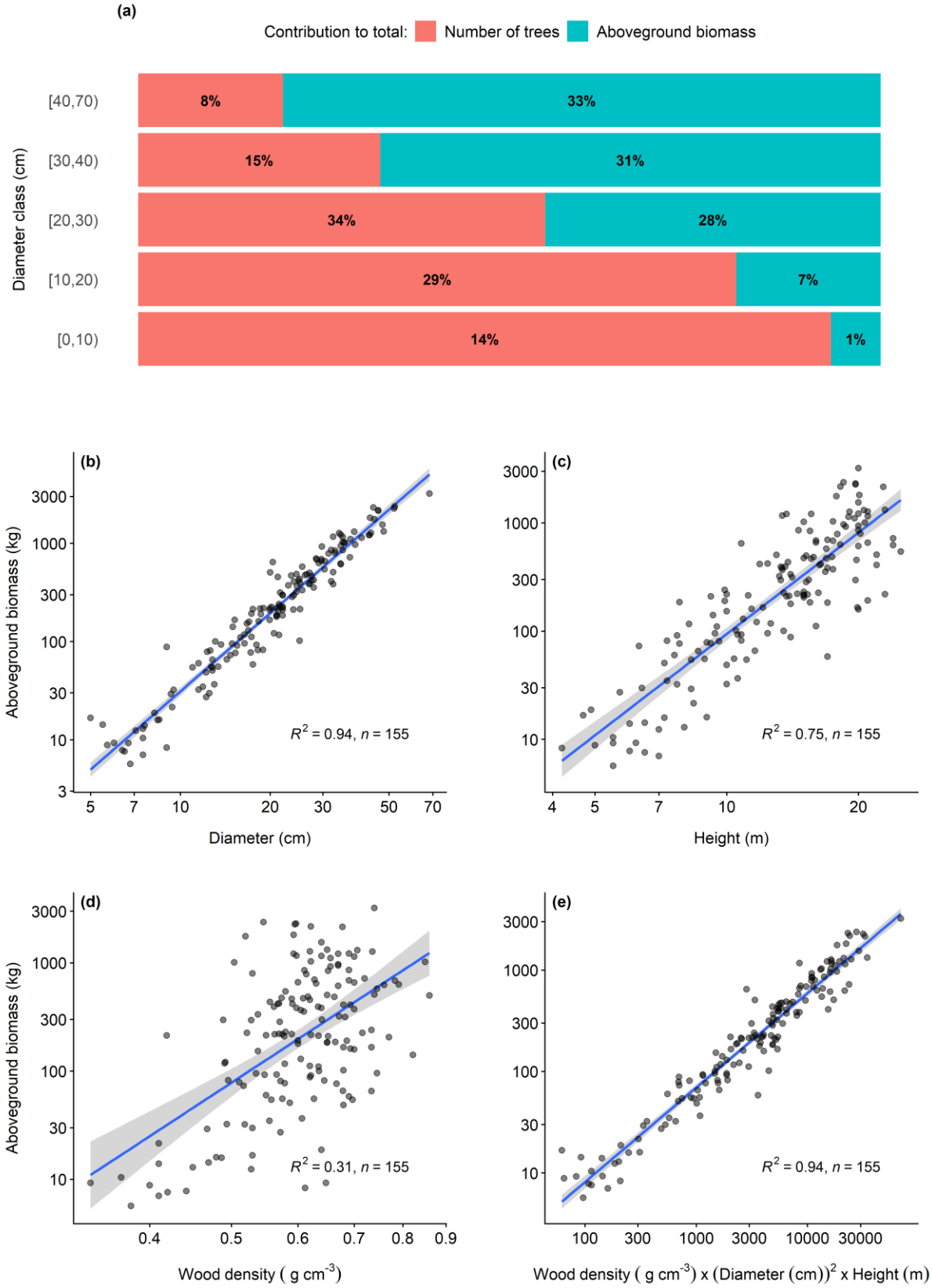


Figure 2. Overview of the tree harvest dataset. The bar plot **(a)** shows the distribution of samples across the five tree diameter classes in terms of both number of trees and their

182 contribution to above ground biomass (*AGB*), both expressed as percentages of the total – Note
183 that the bars in **(a)** are not plotted to scale but merely show the percentage contribution of each
184 *D* class to total number of trees and total *AGB*. Scatterplots show the relationship between *AGB*
185 and the predictors used to model it, including **(b)** stem diameter (*D*), **(c)** total tree height (*H*),
186 **(d)** wood density (ρ) and **(e)** the compound variable of *D*, *H* and ρ. The coefficient of
187 determination (R^2) between *AGB* and each of the predictor variables is shown along with the
188 line of best fit (blue colour) and its 95% confidence bound (grey colour). The dark grey filled
189 circles represent the *AGB* values of each of the 155 destructively harvested trees, plotted on a
190 log-log scale.

191 Apart from the tree harvest datasets used here, there are a number of other studies where
192 destructive sampling for *AGB* has been conducted across miombo woodlands, including those
193 in Mozambique (Ryan et al., 2011; Guedes et al., 2018), Malawi (Kachamba et al., 2016; Kuyah
194 et al., 2016), Tanzania (Chamshama et al., 2004; Mugasha et al., 2013) and Zambia
195 (Chidumayo, 2013b). However, all these datasets lack wood density measurements at the
196 individual tree level and were therefore not suitable to address the core questions of our
197 research.

198 **2.3 Height–diameter modelling data**

199 To determine how different approaches to imputing missing tree height values impact *AGB*
200 estimates, we compiled an additional dataset of trees from miombo woodlands in Zambia for
201 which both *H* and *D* were measured in the field. This included forest inventory data from the
202 three study sites (Mwekera, Miengwe and Katanino) where trees were also destructively
203 harvested to measure *AGB* (Kapinga et al., 2018; Handavu et al., 2021). In Mwekera, 16 square
204 plots (25×25 m) were laid out and all trees with $D \geq 5$ cm in each quadrat were identified to
205 species level. For each tree, *D* was measured to the nearest 0.1 cm using a diameter tape while
206 *H* was measured to the nearest 0.1 m using a Suunto hypsometer (Kapinga et al., 2018). The

same forest inventory approach was used in Miengwe and Katanino forests, although in these two sites circular plots with a 20 m radius were used instead (Handavu et al., 2021). Collectively, *H* and *D* were measured for a total of 4410 trees – excluding the 155 trees which were harvested for *AGB*.

We assessed the data for potential outliers by fitting a log-log linear model relating *H* and *D*. Based on the Cook's distance, a total of 223 trees were flagged as likely measurement errors and were thus excluded from further analysis (Fig. S1b). This left us with 4187 trees for *H-D* model fitting, belonging to 79 tree species and spanning a similar range of tree sizes to those sampled for *AGB* (*D* = 5.0–70 cm; *H* = 2.9–33.0 m) (Table 2).

Table 2: Breakdown of the height-diameter modelling dataset for the three sites in wet miombo woodlands, including number of plots, trees measured, species as well as the median and range of stem diameter at breast height, total tree height, basal area, tree density, elevation, mean total annual precipitation and mean annual temperature. Climate data were extracted from the CHELSA-BIOCLIM+ database (Brun et al., 2022) at a spatial resolution of 30 arc-seconds (approximately 1 km).

Variable	Katanino forest	Miengwe forest	Mwekera forest	Combined dataset
Number of plots	7	55	16	-
Number of trees measured	208	3630	349	4187
Number of species	40	74	33	79
Stem diameter (*D*; cm)	16.0 [5.5 – 51.0]	13.4 [5.0 – 70.0]	20.5 [5.0 – 62.3]	14.0 [5.0 – 70.0]
Tree height (*H*; m)	10.0 [3.3 – 22.0]	9.8 [2.9 – 33.0]	12.5 [3.0 – 25.0]	10.0 [2.9 – 33.0]
Basal area (*BA*; $m^2\ ha^{-1}$)	12.0 [4.9 – 14.8]	15.5 [9.4 – 31.1]	18.1 [10.7 – 29.1]	15.5 [4.9 – 31.1]
Tree density (stems ha^{-1})	342 [104 – 414]	580 [287 – 1329]	416 [224 – 512]	565 [104 – 1329]
Elevation (m a.s.l)	1323 [1255 – 1327]	1324 [1286 – 1340]	1228	1323 [1228 – 1340]
Mean annual precipitation (mm yr^{-1})	1325 [1186 – 1353]	1250 [1130 – 1348]	1198	1249 [1130 – 1353]
Mean annual temperature (°C)	20.1 [20.1 – 20.4]	20.2 [20.1 – 20.5]	20.9	20.2 [20.1 – 20.9]

2.4 Data harmonization and analysis

All data processing and statistical analyses were conducted in R (version 4.3.1; (R Core Team, 2023)) using the brms, GGally, geodata, terra, tidyverse, data.table, ggpmisc, cowplot, multcompView, BIOMASS, rWCVP and U.Taxonstand packages (Bürkner, 2017; Réjou-Méchain et al., 2017; Wickham et al., 2019; Wilke, 2020; Schloerke et al., 2021; Hijmans, 2023; Dowle and Srinivasan, 2023; Brown et al., 2023; Zhang and Qian, 2023; Aphalo, 2024). Prior to conducting statistical analyses, we used the rWCVP and U.Taxonstand packages to harmonize tree species names across all datasets using the World Checklist of Vascular Plants (Govaerts et al., 2021; Brown et al., 2023). For this step, we also cross-referenced and matched species names against the Global Wood Density Database (GWDD) which we used in subsequent analyses to assign ρ values to species using the BIOMASS package (Chave et al., 2009; Réjou-Méchain et al., 2017).

2.5 Objective 1 – Comparing the performance of existing *AGB* models

To determine how much tree-level *AGB* estimates are influenced by the choice of biomass equation, we calculated and compared *AGB* estimates obtained using two existing biomass models. The first *AGB* equation we tested is one of most commonly used pantropical models developed by (Chave et al., 2014), which expresses *AGB* as the following function of *D*, *H* and ρ:

$$AGB = 0.067 \times (\rho D^2 H)^{0.976} \times \exp\left[\frac{0.357^2}{2}\right] \quad (1)$$

where $\exp\left[\frac{0.357^2}{2}\right]$ is the Baskerville correction factor defined as $\frac{\hat{\sigma}^2}{2}$, with $\hat{\sigma}$ corresponding to the estimated residual standard error of the model. The correction factor is used to account for the systematic bias introduced when back-transforming from a log-log linear model to a power law function (Baskerville, 1972). This model was developed using a large collection of tree

harvest data (4004 trees) from across the tropics, including the miombo. It has been used to estimate *AGB* in tropical forests, including the miombo woodlands of Zambia (Pelletier et al., 2018; Kanja et al., 2025).

The second literature model we considered is a local *AGB* model developed as part of Zambia's second integrated land-use assessment (ILUA2) which estimates *AGB* from *D* alone (ILUA, 2016; Forestry Department, 2016):

$$AGB = 0.128 \times D^{2.342} \times \exp\left[\frac{0.299^2}{2}\right] \quad (2)$$

As mentioned previously, there are other *AGB* models developed from destructive samples across miombo woodlands, but for the purpose of this study, we chose eq. 2 for two reasons. First, the model was developed using one of the largest collated tree harvest datasets in the region: 649 out of the 1319 harvested trees in Botswana, Tanzania and Zambia. The trees were harvested in *Acacia*, mopane and miombo vegetation types but with the majority of trees (~85%) coming from dry and wet miombo (Forestry Department, 2016). Further, the dataset used to develop eq. 2 covered the majority of the tree species (73%) that were harvested to measure *AGB* in our study. To our knowledge, all the other existing models developed from destructive samples in the miombo are based on much smaller sample sizes (20–170 harvested trees). Second, this model has been adopted for use at national level in Zambia to estimate *AGB* for all vegetation types (ILUA, 2016), including to generate Zambia's forest reference emission level (FREL) submission to the United Nations Convention for Climate Change (UNFCC) (GRZ, 2016, 2021).

We used eqs. (1) and (2) to estimate the *AGB* for each of the 155 trees using measurements of *D*, *H* and ρ as inputs. We then compared the predictive ability of these two models on the basis of the root mean square error (RMSE, in kg) as a measure of precision, and percentage error (PE, in %) as a measure of bias:

$$\text{RMSE} = \sqrt{\left[\frac{1}{n}\sum_{i=1}^{n}\left(AGB_i - \widehat{AGB_i}\right)^2\right]} \quad (3)$$

$$\text{PE} = \left(\left(\frac{1}{n}\sum_{i=1}^{n}\left(\widehat{AGB_i} - AGB_i\right)\right) / \frac{1}{n}\sum_{i=1}^{n}(AGB_i)\right) \times 100 \quad (4)$$

where AGB_i is the measured AGB for tree i and $\widehat{AGB_i}$ is the predicted AGB for tree i.

We used PE to estimate the magnitude of the mean error relative to the mean observed *AGB*. We chose PE among other metrics of model performance because it gives more weight to large trees, which are the biggest source of uncertainty in *AGB* estimation and contribute disproportionately towards total forest carbon stocks (Fig. 1a; Lutz et al., 2018; Calders et al., 2022).

Finally, we also assessed the performance of the models by fitting a linear regression between observed and predicted *AGB* values and extracting the intercept and slope parameters with their associated 95% confidence intervals. If the model is unbiased, we would expect the intercept to have a value close to 0 and the slope to be approximately 1 (Sileshi, 2014).

2.6 Objective 2 – Reparametrizing *AGB* models to compare their performance to published equations

To complement the two existing *AGB* models, we used the tree harvest dataset described above to reparametrize a miombo-specific version of eqs. 1 and 2. Specifically, we fit linear regressions to log-log transformed data to model the power law relationship between *AGB* and either $\rho D^2 H$ or D alone. Models were fit in a Bayesian framework using the brms package. We used weak priors for the normalization constant (intercept) and scaling exponent (slope), which we assumed to be normally distributed. Parameter estimates were based on 6000 posterior samples drawn from four parallel chains after discarding 1000 burn-in draws per chain. Models were assessed based on the Gelman-Rubin statistic (Rhat = 1.00), the Bulk_ESS and Tail_ESS statistics (both >1000), and posterior predictive checks (Fig. S2), all of which confirmed that

290 the models adequately converged and fitted the observed data well (see Appendix S1 for
291 additional details on model fitting and validation). The resulting fitted models were as follows:

$$AGB = 0.119 \times (\rho D^2 H)^{0.923} \times \exp\left[\frac{0.373^2}{2}\right] \quad (5)$$

$$AGB = 0.083 \times D^{2.590} \times \exp\left[\frac{0.384^2}{2}\right] \quad (6)$$

292 Having reparametrized the two literature *AGB* models (eqs 1 and 2), we then compared
293 the performance of the four equations (1–2 and 5–6) based on RMSE and PE. This allowed us
294 to determine which of the two functional forms is most suitable for predicting *AGB* estimation
295 in miombo woodlands.

296 **2.7 Objective 3 – Influence of height and wood density uncertainty on *AGB* estimates**

297 To better understand how different approaches to imputing H and ρ impact tree-level *AGB*
298 estimates, we devised a series of scenarios in which we imputed values of H and ρ following
299 commonly used practices for dealing with missing data and quantified their relative
300 contribution to *AGB* errors. For the purposes of this analysis, we used the pantropical model of
301 Chave et al. (2014) to predict *AGB* (eq. 1) since it performed well on our dataset (see Results
302 for details) and is widely used by the research community. As above, model performance was
303 assessed by comparing predicted and observed *AGB* values on the basis of RMSE and PE for
304 the entire dataset, as well as PE when grouping trees into different D size classes (<10 cm, 10–
305 20 cm, 20–30 cm, 30–40 cm, >40 cm).

306 As a starting point, we began by using eq. 1 to predict the *AGB* of all the 155 harvested
307 trees when using field-measured values of both H and ρ as inputs. This served as our best case
308 scenario, in which all inputs data have been directly measured in the field. Next, we repeated
309 this same process but replaced field-measured H values with estimates derived from two
310 alternative *H–D* allometries: (1) a locally-calibrated, species-specific allometry and (2) a

311 regional, biome-specific allometry. The local allometry was derived using *H* and *D* values from
312 the 4187 trees described above. The relationship was modelled as a power-law function fit to
313 log–log transformed data ($H = \alpha_j \times D^{\beta_j}$), where both the scaling coefficient (α, intercept) and
314 scaling exponent (β, slope) were allowed to vary across species (j, 79 species + 1 group for 21
315 trees with no species identification) in a hierarchical Bayesian framework. Model fitting and
316 assessment followed the same procedures described above for the reparametrized *AGB* models.
317 Estimated species-level parameters are reported in Table S4, while the population-level fit (or
318 fixed effects) was:

$$H = 1.846 \times D^{0.613} \times \exp\left[\frac{0.240^2}{2}\right] \quad (7)$$

319 For the regional *H–D* allometry, we used an existing model for tropical dry forest trees
320 developed using the Tallo database (Jucker et al., 2022):

$$H = 2.355 \times D^{0.477} \times \exp\left[\frac{0.384^2}{2}\right] \quad (8)$$

321 Finally, we used a similar approach to vary the wood density inputs in the *AGB*
322 equation. Specifically, we replaced field-measured ρ values with either (1) species-specific
323 mean values (or closest taxonomic unit) obtained from the GWDD using the BIOMASS
324 package (Réjou-Méchain et al., 2017) or (2) with a regional mean value for African tropical
325 forests (ρ = 0.598 g cm^{-3}; (Chave et al., 2009)). When matching to the GWDD, 55% of trees
326 were assigned species-level values, 43% genus-level means and the remaining 2% a mean of
327 the dataset (0.682 g cm^{-3}).

328 In total, this gave us nine scenarios to compare: three possible *H* inputs into the *AGB*
329 equation (field-measured, species-specific or biome-specific), three possible wood density
330 inputs (field-measured, species-specific or biome-specific), and their respective combinations
331 (Table 3).

Table 3: Summary of the nine scenarios used to determine the impact of different height and wood density inputs when estimating *AGB*. Uncertainty, in *AGB* estimates, increasing from left to right for height inputs and from top to bottom for wood density.

Scenario 1 Height: measured Wood density: measured Uncertainty: low	**Scenario 2** Height: species-specific *H-D* Wood density: measured Uncertainty: medium	**Scenario 3** Height: regional *H-D* Wood density: measured Uncertainty: medium-high
Scenario 4 Height: measured Wood density: species-specific from GWDD Uncertainty: medium	**Scenario 5** Height: species-specific *H-D* Wood density: species-specific from GWDD Uncertainty: medium-high	**Scenario 6** Height: regional *H-D* Wood density: species-specific from GWDD Uncertainty: high
Scenario 7 Height: measured Wood density: regional mean Uncertainty: medium-high	**Scenario 8** Height: species-specific *H-D* Wood density: regional mean Uncertainty: high	**Scenario 9** Height: regional *H-D* Wood density: regional mean Uncertainty: very high

3. RESULTS

3.1 Objectives 1 and 2 – Uncertainty in *AGB* estimation due to choice of *AGB* model

Of the four *AGB* models we compared, three performed similarly well and produced unbiased estimates of *AGB* across the range of tree sizes (Fig. 3 and Fig. S4): the two models calibrated using the tree harvest data presented in this paper (eqs. 5 and 6) and the existing pantropical model developed by Chave et al. (2014) (eq. 1). In particular, regressions between predicted and observed *AGB* values for both models that used $\rho D^2 H$ as predictors (eqs. 1 and 5) had intercepts with 95% confidence intervals that overlapped with 0 and slopes equal to 1. Of the three *AGB* models that performed similarly well, the reparametrized model with $\rho D^2 H$ as a predictor of *AGB* model had the lowest RMSE (214.2 kg) and PE (-1.6%; Fig. 3c). By contrast,

346 the ILUA2 model (eq. 2) developed as part of Zambia's forest inventory program substantially
347 underestimated *AGB* and had the worst performance metrics (RMSE = 305.7kg and PE = -
348 36.3%) (Fig. 3b), especially for large trees (blue line in Fig. 3f; see also Fig. S4). On average,
349 predicted values of *AGB* obtained using the ILUA2 model were around 35% lower than those
350 measured in the field (slope coefficient = 1.5; Fig. 3b) and trees in the largest size class had a
351 PE of -37% (Fig. 3f).

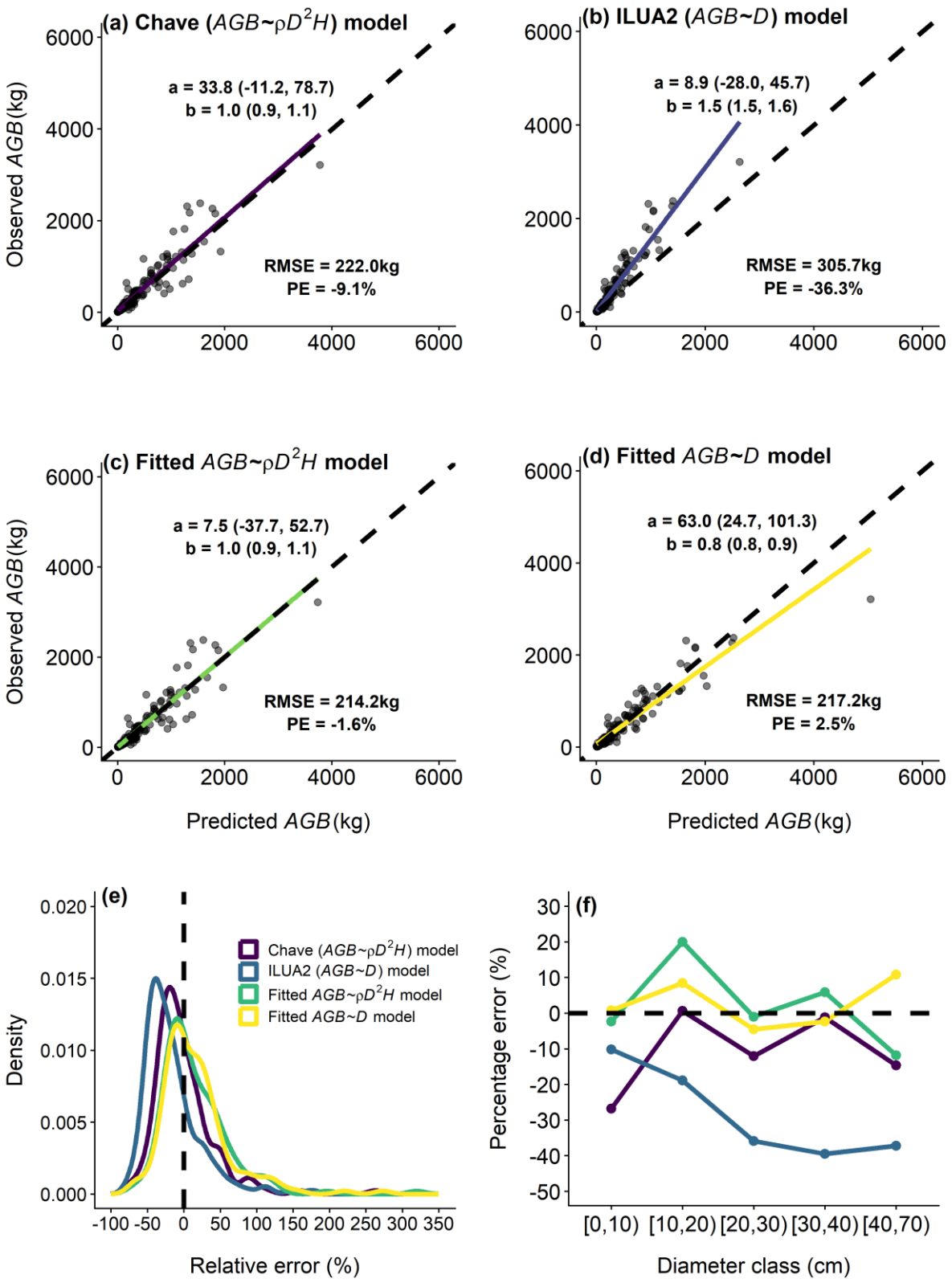


Figure 3. Predictive accuracy of the four alternative aboveground biomass (*AGB*) models. Scatterplots **(a–d)** show the relationship between observed and predicted *AGB* values across

355 the 155 trees included in the dataset. Coloured lines correspond to the fit of a linear model
356 between observed and predicted *AGB* values, while dashed lines illustrate a 1:1 relationship.
357 Fit statistics for each model are reported in the panels, including the intercept, **a**, and slope ,**b**,
358 of the regression line with 95% confidence intervals in brackets. Model errors are visualised in
359 the bottom two panels, including **(e)** the distribution of relative errors, as a percentage,
360 (calculated as: $((\widehat{AGB}_i - AGB_i)/AGB_i) \times 100$; where AGB_i is the measured AGB for tree i;
361 and $\widehat{AGB}_i$ is the estimated AGB for tree i) for each of the four models and (**f**) the percentage
362 error (PE, in %) of trees grouped into five stem diameter classes.

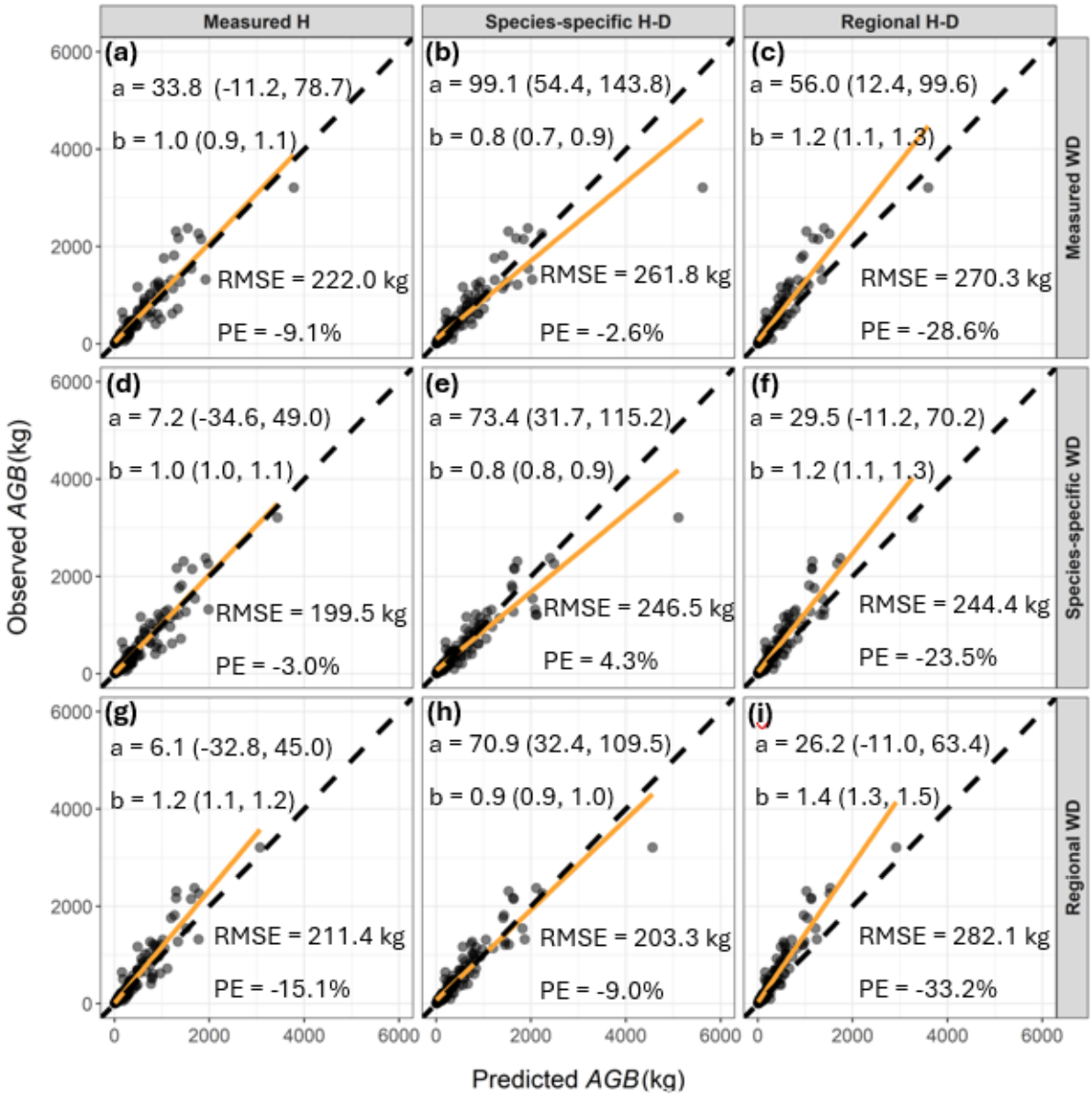
363 **3.2 Objective 3 – Error in *AGB* estimation due to uncertainty in height and wood**
364 **density**

365 Across the nine scenarios in which we modified height (H) and wood density (ρ) inputs in the
366 pantropical *AGB* model, we found that replacing field-measured values of H and ρ with species-
367 specific estimates did not substantially worsen *AGB* estimates (Figs 4–5). In particular, height
368 estimates obtained using the locally-calibrated, species-specific *H–D* allometry (eq. 7) were
369 statistically indistinguishable (Fig. S5a) from those measured in the field and consequently had
370 little impact on predicted *AGB* values (PE = -2.6% and RMSE = 261.8 kg; Fig. 4b). Similarly,
371 while species-specific wood density values obtained from the GWDD were significantly higher
372 (Fig. S5b) than those measured on the destructively harvested trees, their use in the *AGB* model
373 had almost no impact on *AGB* estimation (PE = -3.0% and RMSE = 199.5 kg, with a slope
374 coefficient of 1.0 when comparing predicted and observed values of *AGB*; Fig. 4d).

375 By contrast, when H and ρ values were replaced with coarser regional-level estimates,
376 errors in *AGB* increased substantially. This was most pronounced for scenarios that involved
377 using height estimates derived from the regional *H–D* allometry for tropical dry forests (eq. 8;
378 Fig. 4c,f,i). Because this allometry severely underestimated tree heights by several meters

379 (Figs. 6 and S6), its use led to a nearly 30% underestimation of *AGB* (slope coefficient between
380 observed and predicted values = 1.2; Fig. 4c). A similar, albeit much weaker trend was also
381 observed for wood density. The regional mean ρ value for African tropical forests was only
382 slightly lower than the mean ρ value of species sampled in our study (0.598 vs 0.607 g cm^{-3}).
383 Therefore, replacing field-measured ρ values with a regional mean resulted in a slight increase
384 in underestimation of *AGB* (PE = -15.1% and slope coefficient = 1.2; Fig. 4g). When these two
385 sources of errors were combined, they compounded each other and led to an underestimation
386 of *AGB* that was comparable in magnitude to that of using the ILUA2 model to estimate *AGB*
387 instead of the pantropical equation of Chave et al. (2014) (PE = -33.2%, RMSE = 282.1 kg and
388 slope coefficient = 1.4; Fig. 4i).

389

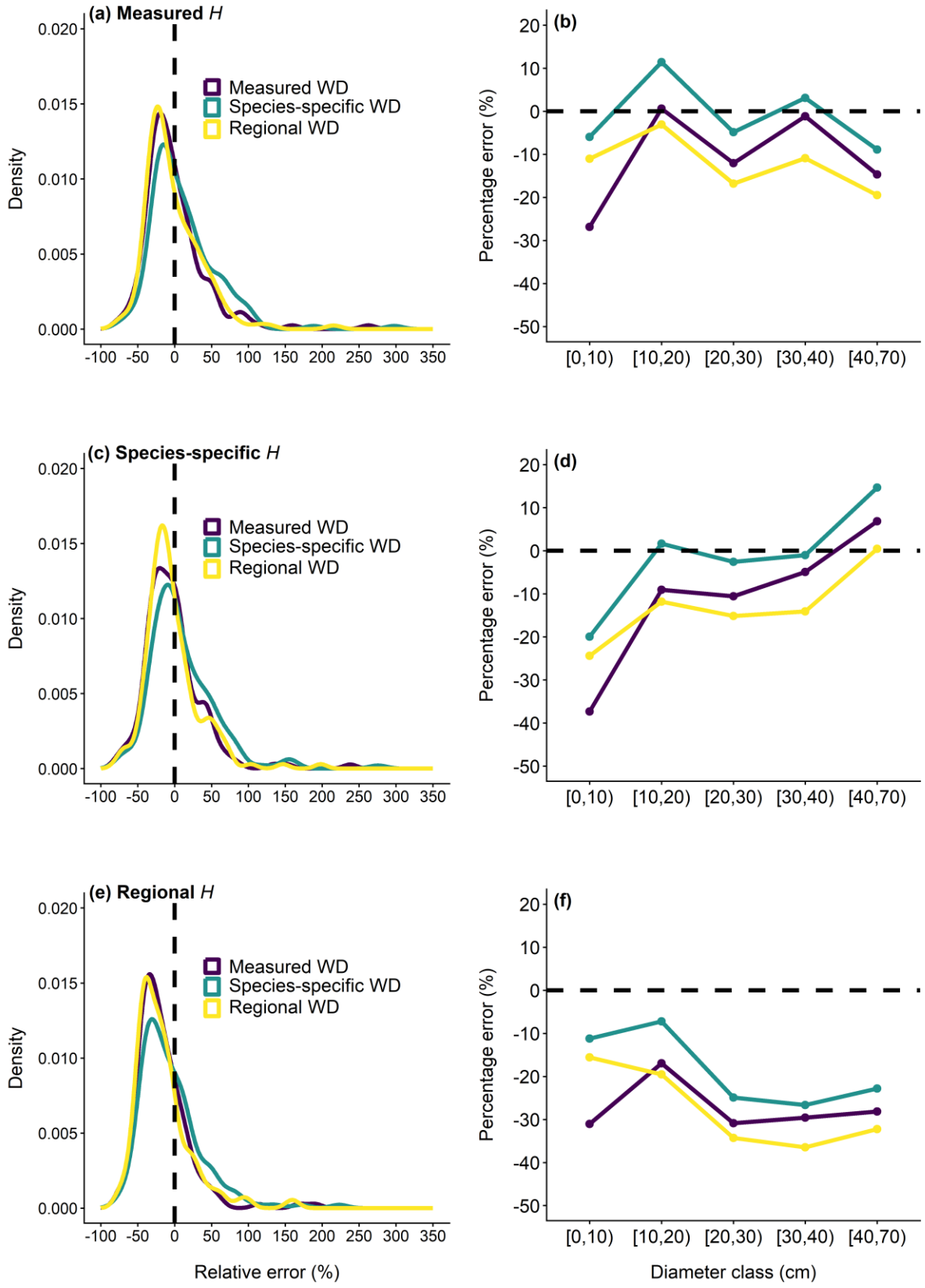


390

391 **Figure 4.** Errors in aboveground biomass (*AGB*) estimation arising from uncertainty in tree
392 height (*H*) and wood density (ρ). Each panel corresponds to one of the nine scenarios described
393 in Table 3 in which we altered inputs of *H* and ρ in the *AGB* model developed by Chave et al.
394 (2014). *H* inputs vary in uncertainty from left to right, from field measured, to those estimated
395 using a species-specific *H-D* model (eq. 7), and finally those derived from a regional *H-D*
396 model (eq. 8). ρ inputs vary in uncertainty from top to bottom, from field measured ρ values,
397 to species-specific (or closest taxonomic unit) mean values derived from the Global Wood
398 Density Database, and finally those based on a single regional mean value for African tropical

399 forests derived from the literature. The orange coloured solid lines correspond to the fit of a
400 linear model between observed and predicted *AGB* values, while dashed lines illustrate a 1:1
401 relationship. Fit statistics for each model are reported in the panels, including the intercept (a)
402 and slope (b) of the regression line (with 95% confidence intervals in brackets), as well as the
403 RMSE and PE. Refer to Fig. S8 for a similar plot but excluding the largest observed/predicted
404 *AGB* value which , by visual inspection, appears like an outlier when compared to other data
405 values.

406

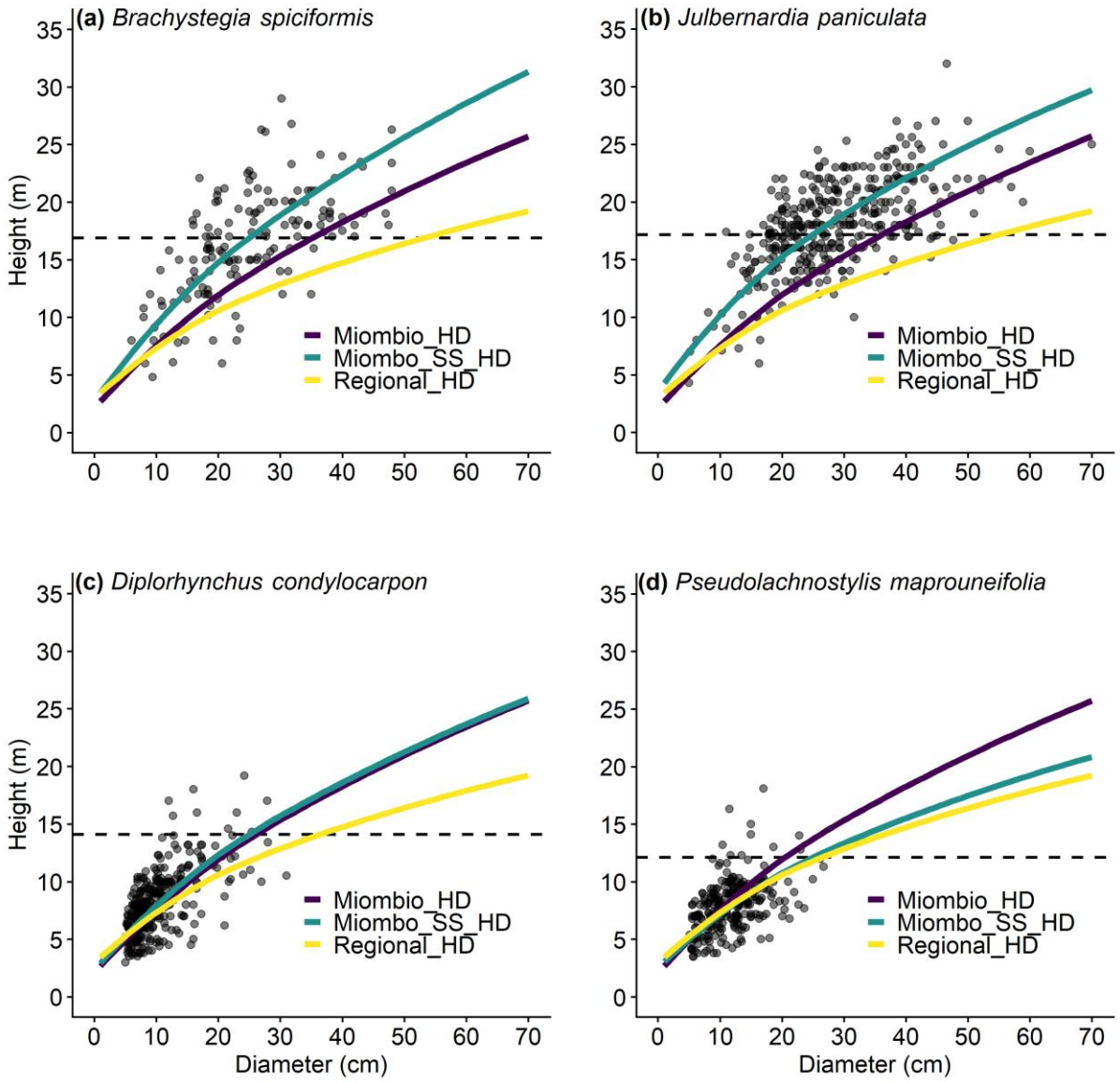

(a) Measured H
(b)
(c) Species-specific H
(d)
(e) Regional H
(f)
Measured WD
Species-specific WD
Regional WD
Density
Percentage error (%)
Relative error (%)
Diameter class (cm)
[0,10)
[10,20)
[20,30)
[30,40)
[40,70)

407

408

409

410 **Figure 5.** Errors in aboveground biomass (*AGB*) estimation due to uncertainty in tree height
411 (*H*) and wood density (ρ) across the nine scenarios depicted in Table 3. Panels on the left show
412 the distribution of relative errors, as a percentage, (calculated as: $((\widehat{AGB}_i - AGB_i)/AGB_i) \times$
413 100; where AGB_i is the measured AGB for tree i; and $\widehat{AGB}_i$ is the estimated AGB for tree i) in
414 *AGB* across the nine scenarios, while those on the right show the percentage error (PE, in %)
415 for trees grouped into the five stem diameter classes across scenarios. In all cases, *AGB* was
416 estimated using the pan-tropical model developed by Chave et al. (2014). Species-specific *H*
417 (Fig. 5c) refers to using eq. 7 to estimate tree H while regional *H* (Fig. 5e) corresponds to using
418 eq. 8 to estimate tree *H*.



419

420 **Figure 6.** Variability in height-diameter (*H-D*) relationships among common miombo tree
421 species with differing adult statures. Fitted lines correspond to the population-level fit of eq.
422 7(purple), the species-level deviations from the population-level fit (green; see Table S4 for
423 species-level parameter values), and the fit of the regional *H-D* allometry derived from the
424 Tallo database (yellow; eq. 8). The horizontal dashed black lines show the height prediction for
425 a tree with diameter of 25 cm using the species-specific *H-D* model.

4. DISCUSSION

4.1 Strength in numbers: pantropical model provides robust estimates of *AGB*

Our study shows that when accurate measurements or estimates of tree height and wood density are available, the pantropical model developed by Chave et al. (2014) can generate unbiased estimates of *AGB*. In fact in our case, this pantropical model performed similarly well to *AGB* equations calibrated against new data (Fig. 3 and Fig. S4). A key feature of this pantropical model is that compared to other regional or species-specific models that exist in the literature, it was developed using a large number of harvested trees (>4000) that span a broad range of environments and sizes. This is clearly a major strength when it comes to making predictions against new data. A priority for future research in this field should therefore be to further consolidate and expand data on harvested trees into a common database so that robust and widely applicable *AGB* models can be built.

By contrast, we found that the regional ILUA2 model developed to predict *AGB* for Zambia's forests as part of the national forest inventory severely underestimated *AGB*, particularly that of large trees. There are two plausible reasons for this underestimation. First, although the ILUA2 model was developed using 649 harvested trees, these comprised mostly small to medium size trees ($D \leq 30$cm) (Forestry Department, 2016). Small sample sizes and/or large sample sizes with mostly smaller trees to parameterize *AGB* models have been identified as major sources of *AGB* errors and uncertainty (Chave et al., 2004). Second, the ILUA2 model uses *D* as the sole predictor of *AGB*. While *D* is clearly the single strongest correlate of *AGB* (Fig. 1b), in doing so the model does not account for differences in *H-D* scaling among species (Fig. 6) and forest types (Timberlake et al., 2010; Munalula et al., 2020; Yambayamba et al., 2025), nor does it incorporate variability in wood density which can substantially affect *AGB* estimates (Mitchard et al., 2014; Jucker et al., 2018; Phillips et al., 2019). Our findings align with a recent study in the same region suggesting that commonly applied allometric models

451 underestimate *AGB* of miombo woodlands (Demol et al., 2024). This has important practical
452 implications, including reporting and verification of forest carbon stocks and dynamics under
453 REDD+ and emerging carbon trading initiatives (Köhl et al., 2020; GRZ, 2021; Melo et al.,
454 2023), as well as the calibration and validation of satellite-derived estimates of forest carbon
455 stocks. For instance, Zambia has previously used the ILUA2 model to estimate FREL
456 submissions to the UNFCCC (GRZ, 2016) but most recently identified the pantropical model
457 for consideration (GRZ, 2021). In this respect, our study highlights the challenges associated
458 with accurate estimation of *AGB* stocks and therefore underscores the need for rigorous
459 methods for quantifying *AGB* stocks and dynamics in miombo woodlands and beyond.

460 **4.2 Tree height uncertainty can severely bias *AGB* estimates**

461 Our study reiterates the recommendation of previous works to account for tree height when
462 estimating *AGB* (Feldpausch et al., 2012; Chave et al., 2014; Djomo et al., 2016; Handavu et
463 al., 2021). However, our results also underscore how the inclusion of *H* in *AGB* models is not
464 without its challenges (Chave et al., 2014; Kapinga et al., 2018). First, conventional field
465 measurements of *H* are not only time consuming to take but also prone to errors, especially for
466 large trees and in closed canopies (Larjavaara and Muller-Landau, 2013; Wang et al., 2019).
467 Second, the common practice of using *H-D* models to estimate tree height when this is not
468 measured is equally subject to errors, especially where locally fitted *H-D* models are
469 unavailable (Fayolle et al., 2016; Sullivan et al., 2018). In line with previous studies, our results
470 demonstrate the peril of applying generic and regional *H-D* models to specific locations that
471 are environmentally or taxonomically distinct (Feldpausch et al., 2012; Kearsley et al., 2013;
472 Molto et al., 2014; Ledo et al., 2016; Fayolle et al., 2016). Using a regional *H-D* model
473 developed for tropical dry forests led to a severe underestimation of *AGB*. Worse still, this
474 underestimation increased with *D* (Fig. 5f), which is particularly undesirable since larger trees
475 contribute disproportionately to total forest carbon stocks (Fig. 1a; (Lutz et al., 2018)). Our

476 approach of fitting a locally-calibrated and species-specific *H-D* model substantially improved
477 the accuracy of *AGB* estimates. However, access to high-quality local datasets to parameterize
478 such allometries is often limited (Jucker et al., 2022).

479 The importance of tree height in *AGB* estimation has also been demonstrated in studies
480 using remote sensing methods to map forest structure. For example, detailed reconstructions of
481 tree architecture made possible by terrestrial laser scanning have shown that traditional
482 allometric models can underestimate tree height and therefore *AGB* (Calders et al., 2022;
483 Terryn et al., 2024). Given the obvious challenges associated with accurate measurement of *H*
484 using conventional field methods, we argue that improvement in *AGB* estimation in miombo
485 woodlands requires leveraging increasingly available and affordable remote sensing
486 technologies such as LiDAR (Momo Takoudjou et al., 2018; Calders et al., 2022; Demol et al.,
487 2022; Demol et al., 2024). These data provide a robust way to characterise the 3D architecture
488 of trees that can be used to describe forest structure, functioning and dynamics with greater
489 accuracy and across larger scales than traditional field methods (Jucker et al., 2023; Battison
490 et al., 2024).

491 **4.3 The importance of accounting for wood density when estimating *AGB***

492 Wood density can vary considerably among tree species, with values ranging almost three fold
493 from as low as 0.34 g cm^{-3} to 0.86 g cm^{-3} across those sampled in our study. As previous work
494 in Amazonia has shown, failure to properly account for this variability in wood density among
495 species and forest types can severely bias large-scale estimates of forest carbon stocks inferred
496 via remote sensing (Mitchard et al., 2014; Phillips et al., 2019). In the case of the miombo
497 woodlands studied here, uncertainty in wood density was of secondary importance to that in
498 tree height in driving errors in *AGB* estimation. But this is likely to differ among forest types
499 and will depend on both the accuracy of available *H–D* allometries and the coverage of wood
500 density databases like the GWDD.

When field-measured values of wood density were replaced with ones obtained from the GWDD, we found that overall wood density was overestimated across the population. This led to only a modest reduction in underestimation of *AGB*, as wood density values from the GWDD were generally correlated to those measured in the field (Fig. S7). This confirms previous work showing that while wood density can vary somewhat within species, it is generally quite a conserved trait (Chave et al., 2009; Fischer et al., 2026). Therefore, provided trees have been identified to species level and that these species have matching observations in the GWDD, our results suggest that *AGB* can be estimated with limited bias. This provides a strong incentive to continue to curate and expand field reference collections of wood density to support large-scale mapping of forest carbon stocks (Fischer et al., 2026). In the context of Zambia's miombo woodlands, only 31 tree species (out of approximately 238 species identified in the most recent national forest inventory (Pelletier et al., 2018; Yambayamba et al., 2025)) have wood density records (Forestry Department, 2016), making it imperative that taxonomic coverage is increased in the future.

Uncertainty in wood density can compound the errors in *AGB* associated with the use of a generic *H–D* allometry, but it is easy to imagine a situation in which these errors could instead cancel each other out, making them even harder to detect and quantify. In this regard, our framework provides a simple and robust way to decompose errors in *AGB* arising from uncertainty in both height and wood density. Replicating this analysis on a larger dataset, such as the pantropical *AGB* database developed by Chave et al. (2014), would provide valuable insights into the main sources of error in *AGB* estimation and how these vary across forest types and biogeographic regions.

5. CONCLUSION

Our study aimed at comparing the predictive performance of existing and reparametrized *AGB* models in miombo woodlands and quantifying the errors associated with using different approaches to imputing of height and wood density. We have shown that using *AGB* models that incorporate *H* and ρ, in addition to *D*, provide better and more transferable estimates than those that rely exclusively on *D*. The reparametrized model of Chave et al. (2014) we develop here thus provides a good starting point for improving *AGB* estimates in miombo woodlands. However, looking ahead, we encourage the research community to continue to move towards larger, integrated databases of tree *AGB* in order to develop generalised models that can underpin accurate accounting of forest carbon stocks under REDD+ and carbon trading initiatives.

Our study further revealed that uncertainty in *H* (more than in ρ in the miombo) can lead to substantial errors in *AGB* estimates. Since *H* is typically only measured for a small sub-sample of trees and mostly estimated using *H-D* models in conventional forest inventories, we therefore reiterate that great care is needed when selecting the approach to estimate *H* (particularly if locally available *H* data are not available to assess model performance). Collating and curating accurately measured *H-D* data and developing local species-specific *H-D* allometries remain a priority for the miombo and many other regions (particularly those in the tropics). The species-specific *H-D* models we develop here thus serve as a baseline for improving *AGB* estimation in miombo woodlands, although future work should also consider comparing different functional forms for modelling *H-D* relationships (Cano et al., 2019).

The *AGB* and *H-D* allometries developed in this study will hopefully serve as a blueprint for improving the characterization and modelling of tree allometry, ecosystem function and biomass estimation in miombo woodlands. In particular, emerging remote sensing technologies such as terrestrial and airborne LiDAR are increasingly being used to characterize

548 tree structure and map landscape-scale carbon stocks, but require field based approaches for
549 validation and calibration (Jucker et al., 2017; Chave et al., 2019). Similarly, improved
550 allometries are crucial to accurate simulation of vegetation response to environmental change
551 in dynamic global vegetation models (Fischer et al., 2019).

552

ACKNOWLEDGEMENTS

Arthur M. Yambayamba (AMY) was supported by a PhD scholarship through the Commonwealth Scholarship Commission (CSC) programme (grant: ZMCS-2021-542). Tommaso Jucker (TJ) was supported by a NERC Independent Research Fellowship (grant: NE/S01537X/1) and through a UKRI Frontier Research grant (grant: EP/Y003810/1) that also supported AMY.

AUTHOR CONTRIBUTIONS

AMY and TJ designed the study. Kondwani Kapinga (KK) did the vegetation assessment, forest inventory, destructive sampling and laboratory analysis for the Mwekera forest dataset. Ferdinand Handavu (FH) did the vegetation assessment, forest inventory, destructive sampling and laboratory analysis, with assistance from KK, for the Katanino and Miengwe forests datasets. AMY did the data collating and led the analysis with assistance from TJ. AMY wrote the first draft of the manuscript with all the authors contributing substantially to revisions.

CONFLICT OF INTEREST

The authors declare no competing interests.

DATA AND CODE AVAILABILITY STATEMENT

The aboveground biomass and height-diameter data used in this study are publicly archived on Zenodo (https://doi.org/10.5281/zenodo.22307029), with the exception of the data from the Katanino and Miengwe sites, which are available upon request from the second author. Species-level wood density values were obtained from the Global Wood Density Database: https://zenodo.org/records/20815517. All R codes used for the analysis are available upon request from the corresponding author.

SUPPLEMENTARY MATERIAL

Additional supporting information may be found online in the Supporting Information section.

REFERENCES

Aphalo, P.: _ggpmisc: Miscellaneous Extensions to 'ggplot2'_. R package version 0.6.0,, <https://CRAN.R-project.org/package=ggpmisc>. 2024.

Arias, P. A., N. Bellouin, E. Coppola, R.G. Jones, G. Krinner, J. Marotzke, V. Naik, M.D. Palmer, G.-K. Plattner, J.Rogelj, M. Rojas, J. Sillmann, T. Storelvmo, P.W. Thorne, B. Trewin, K. Achuta Rao, B. Adhikary, R.P. Allan, K.Armour, G. Bala, R. Barimalala, S. Berger, J.G. Canadell, C. Cassou, A. Cherchi, W. Collins, W.D. Collins, S.L. Connors, S. Corti, F. Cruz, F.J. Dentener, C. Dereczynski, A. Di Luca, A. Diongue Niang, F.J. Doblas-Reyes, A. Dosio, H. Douville, F. Engelbrecht, V. Eyring, E. Fischer, P. Forster, B. Fox-Kemper, J.S. Fuglestvedt, J.C. Fyfe, N.P. Gillett, L. Goldfarb, I. Gorodetskaya, J.M. Gutierrez, R. Hamdi, E. Hawkins, H.T. Hewitt, P. Hope, A.S. Islam, C. Jones, D.S. Kaufman, R.E. Kopp, Y. Kosaka, J. Kossin, S. Krakovska, J.-Y. Lee, J. Li, T. Mauritsen, T.K. Maycock, M. Meinshausen, S.-K. Min, P.M.S. Monteiro, T. Ngo-Duc, F. Otto, I. Pinto, A. Pirani, K. Raghavan, R. Ranasinghe, A.C. Ruane, L. Ruiz, J.-B. Sallée, B.H. Samset, S. Sathyendranath, S.I. Seneviratne, A.A. Sörensson, S. Szopa, I. Takayabu, A.-M. Tréguier, B. van den Hurk, R. Vautard, K. von Schuckmann, S. Zaehle, X. Zhang, and K. Zickfeld: Climate Change 2021: The Physical Science Basis. Contribution of Working Group I to the Sixth Assessment Report of the Intergovernmental Panel on Climate Change; Technical Summary, in, edited by: Masson-Delmotte, V., P. Zhai, A. Pirani, S.L. Connors, C. Péan, S. Berger, N. Caud, Y. Chen, L. Goldfarb, M.I. Gomis, M. Huang, K. Leitzell, E. Lonnoy, J.B.R., Matthews, T.K. Maycock, T. Waterfield, O. Yelekçi, R. Yu, and Zhou, B., Cambridge University Press, Cambridge, United Kingdom and New York, NY, USA , pp. 33−144, doi:10.1017/9781009157896.002., 33-144, 10.1017/9781009157896.002, 2021.

Banin, L., Feldpausch, T. R., Phillips, O. L., Baker, T. R., Lloyd, J., Affum-Baffoe, K., Arets, E., Berry, N. J., Bradford, M., and Brienen, R. J. W.: What controls tropical forest architecture? Testing environmental, structural and floristic drivers, Global Ecology and Biogeography, 21, 1179-1190, 2012.

Baskerville, G.: Use of logarithmic regression in the estimation of plant biomass, Canadian Journal of Forest Research, 2, 49-53, 1972.

606 Battison, R., Prober, S. M., Zdunic, K., Jackson, T. D., Fischer, F. J., and Jucker, T.: Tracking
607 tree demography and forest dynamics at scale using remote sensing, New Phytologist, 244,
608 2251-2266, 2024.

609 Bomfim, B., Pinagé, E. R., Emmert, F., and Kueppers, L. M.: Improving sustainable tropical
610 forest management with voluntary carbon markets, Plant and Soil, 1-8, 2022.

611 Brown, M. J. M., Walker, B. E., Black, N., Govaerts, R. H. A., Ondo, I., Turner, R., and Nic
612 Lughadha, E.: rWCVP: a companion R package for the World Checklist of Vascular Plants,
613 New Phytologist, 240, 1355-1365, https://doi.org/10.1111/nph.18919, 2023.

614 Brun, P., Zimmermann, N. E., Hari, C., Pellissier, L., and Karger, D. N.: Global climate-related
615 predictors at kilometre resolution for the past and future, Earth Syst. Sci. Data Discuss., 2022,
616 1-44, 10.5194/essd-2022-212, 2022.

617 Bürkner, P.-C.: brms: An R Package for Bayesian Multilevel Models Using Stan, Journal of
618 Statistical Software, 80, 1 - 28, 10.18637/jss.v080.i01, 2017.

619 Calders, K., Verbeeck, H., Burt, A., Origo, N., Nightingale, J., Malhi, Y., Wilkes, P., Raumonen,
620 P., Bunce, R. G. H., and Disney, M.: Laser scanning reveals potential underestimation of
621 biomass carbon in temperate forest, Ecological Solutions and Evidence, 3, e12197,
622 https://doi.org/10.1002/2688-8319.12197, 2022.

623 Cano, M. I., Muller-Landau, H. C., Wright, S. J., Bohlman, S. A., and Pacala, S. W.: Tropical
624 tree height and crown allometries for the Barro Colorado Nature Monument, Panama: a
625 comparison of alternative hierarchical models incorporating interspecific variation in relation
626 to life history traits, Biogeosciences, 16, 847-862, 2019.

627 Chamshama, S., Mugasha, A., and Zahabu, E.: Stand biomass and volume estimation for
628 Miombo woodlands at Kitulangalo, Morogoro, Tanzania, The Southern African Forestry
629 Journal, 200, 59-70, 2004.

630 Chave, J., Condit, R., Aguilar, S., Hernandez, A., Lao, S., and Perez, R.: Error propagation and
631 scaling for tropical forest biomass estimates, Philosophical Transactions of the Royal Society
632 of London. Series B: Biological Sciences, 359, 409-420, 2004.

633 Chave, J., Coomes, D., Jansen, S., Lewis, S. L., Swenson, N. G., and Zanne, A. E.: Towards a
634 worldwide wood economics spectrum, Ecology letters, 12, 351-366, 2009.

635 Chave, J., Davies, S. J., Phillips, O. L., Lewis, S. L., Sist, P., Schepaschenko, D., Armston, J.,
636 Baker, T. R., Coomes, D., and Disney, M.: Ground data are essential for biomass remote sensing
637 missions, Surveys in Geophysics, 1-18, 2019.

638 Chave, J., Réjou-Méchain, M., Búrquez, A., Chidumayo, E., Colgan, M. S., Delitti, W. B. C.,
639 Duque, A., Eid, T., Fearnside, P. M., and Goodman, R. C.: Improved allometric models to
640 estimate the aboveground biomass of tropical trees, Global change biology, 20, 3177-3190,
641 2014.

642 Chidumayo, E.: Development of Brachystegia-Julbernardia woodland after clear-felling in
643 central Zambia: Evidence for high resilience, Applied Vegetation Science, 7, 237-242, 2004.

644 Chidumayo, E. N.: Forest degradation and recovery in a miombo woodland landscape in
645 Zambia: 22 years of observations on permanent sample plots, Forest Ecology and Management,
646 291, 154-161, 2013a.

647 Chidumayo, E. N.: Estimating tree biomass and changes in root biomass following clear-
648 cutting of Brachystegia-Julbernardia (miombo) woodland in central Zambia, Environmental
649 conservation, 41, 54-63, 2013b.

650 Chojnacky, D. C., Heath, L. S., and Jenkins, J. C.: Updated generalized biomass equations for
651 North American tree species, Forestry, 87, 129-151, 2014.

652 Clark, D. B. and Kellner, J. R.: Tropical forest biomass estimation and the fallacy of misplaced
653 concreteness, Journal of Vegetation Science, 23, 1191-1196, 2012.

654 Colgan, M. S., Asner, G. P., and Swemmer, T.: Harvesting tree biomass at the stand level to
655 assess the accuracy of field and airborne biomass estimation in savannas, Ecological
656 Applications, 23, 1170-1184, https://doi.org/10.1890/12-0922.1, 2013.

657 Demol, M., Verbeeck, H., Gielen, B., Armston, J., Burt, A., Disney, M., Duncanson, L.,
658 Hackenberg, J., Kükenbrink, D., and Lau, A.: Estimating forest above-ground biomass with
659 terrestrial laser scanning: Current status and future directions, Methods in Ecology and
660 Evolution, 13, 1628-1639, 2022.

661 Demol, M., Aguilar-Amuchastegui, N., Bernotaite, G., Disney, M., Duncanson, L., Elmendorp,
662 E., Espejo, A., Furey, A., Hancock, S., Hansen, J., Horsley, H., Langa, S., Liang, M., Locke,
663 A., Manjate, V., Mapanga, F., Omidvar, H., Parsons, A., Peneva-Reed, E., Perry, T., Puma Vilca,
664 B. L., Rodríguez-Veiga, P., Sutcliffe, C., Upham, R., de Walque, B., and Burt, A.: Multi-scale

lidar measurements suggest miombo woodlands contain substantially more carbon than thought, Communications Earth & Environment, 5, 366, 10.1038/s43247-024-01448-x, 2024.

Djomo, A. N., Picard, N., Fayolle, A., Henry, M., Ngomanda, A., Ploton, P., McLellan, J., Saborowski, J., Adamou, I., and Lejeune, P.: Tree allometry for estimation of carbon stocks in African tropical forests, Forestry: An International Journal of Forest Research, 89, 446-455, 2016.

Dowle, M. and Srinivasan, A.: _data.table: Extension of `data.frame`_ R package version 1.14.8, <https://CRAN.R-project.org/package=data.table>, 2023.

Dubayah, R., Blair, J. B., Goetz, S., Fatoyinbo, L., Hansen, M., Healey, S., Hofton, M., Hurtt, G., Kellner, J., Luthcke, S., Armston, J., Tang, H., Duncanson, L., Hancock, S., Jantz, P., Marselis, S., Patterson, P. L., Qi, W., and Silva, C.: The Global Ecosystem Dynamics Investigation: High-resolution laser ranging of the Earth's forests and topography, Science of Remote Sensing, 1, 100002, https://doi.org/10.1016/j.srs.2020.100002, 2020.

Dziba, L., Ramoelo, A., Ryan, C., Harrison, S., Pritchard, R., Tripathi, H., Sitas, N., Selomane, O., Engelbrecht, F., Pereira, L., Katerere, Y., Chirwa, P. W., Ribeiro, N. S., and Grundy, I. M.: Scenarios for Just and Sustainable Futures in the Miombo Woodlands, in: Miombo Woodlands in a Changing Environment: Securing the Resilience and Sustainability of People and Woodlands, edited by: Ribeiro, N. S., Katerere, Y., Chirwa, P. W., and Grundy, I. M., Springer International Publishing, Cham, 191-234, 10.1007/978-3-030-50104-4_6, 2020.

Ellis, E. C., Gauthier, N., Klein Goldewijk, K., Bliege Bird, R., Boivin, N., Díaz, S., Fuller, D. Q., Gill, J. L., Kaplan, J. O., Kingston, N., Locke, H., McMichael, C. N. H., Ranco, D., Rick, T. C., Shaw, M. R., Stephens, L., Svenning, J.-C., and Watson, J. E. M.: People have shaped most of terrestrial nature for at least 12,000 years, Proceedings of the National Academy of Sciences, 118, e2023483118, doi:10.1073/pnas.2023483118, 2021.

Fareed, N. and Numata, I.: Evaluating the impact of field-measured tree height errors correction on aboveground biomass modeling using airborne laser scanning and GEDI datasets in Brazilian Amazonia, Trees, Forests and People, 100751, https://doi.org/10.1016/j.tfp.2024.100751, 2024.

Fayolle, A., Panzou, G. J. L., Drouet, T., Swaine, M. D., Bauwens, S., Vleminckx, J., Biwole, A., Lejeune, P., and Doucet, J.-L.: Taller trees, denser stands and greater biomass in semi-

695 deciduous than in evergreen lowland central African forests, Forest Ecology and Management,
696 374, 42-50, 2016.

697 Feldpausch, T. R., Banin, L., Phillips, O. L., Baker, T. R., Lewis, S. L., Quesada, C. A., Affum-
698 Baffoe, K., Arets, E. J. M. M., Berry, N. J., and Bird, M.: Height-diameter allometry of tropical
699 forest trees, Biogeosciences, 2011.

700 Feldpausch, T. R., Lloyd, J., Lewis, S. L., Brienen, R. J., Gloor, M., Monteagudo Mendoza, A.,
701 Lopez-Gonzalez, G., Banin, L., Abu Salim, K., and Affum-Baffoe, K.: Tree height integrated
702 into pantropical forest biomass estimates, Biogeosciences, 3381-3403, 2012.

703 Fischer, F. J., Maréchaux, I., and Chave, J.: Improving plant allometry by fusing forest models
704 and remote sensing, New Phytologist, 223, 1159-1165, 2019.

705 Fischer, F. J., Chave, J., Zanne, A., Jucker, T., Fajardo, A., Fayolle, A., de Lima, R. A. F.,
706 Vieilledent, G., Beeckman, H., Hubau, W., De Mil, T., Wallenus, D., Aldana, A. M., Alvarez-
707 Dávila, E., Alves, L. F., Apgaua, D. M. G., Arcanjo, F., Bastin, J.-F., Bilous, A., Birnbaum, P.,
708 Blyshchyk, V., Borah, J., Boukili, V., Camarero, J. J., Casas, L., Cazzolla Gatti, R., Chambers,
709 J. Q., Fabiano, E. C., Choat, B., Conti, G., Cornwell, W., Dar, J. A., Das, A. K., Dobler, M.,
710 Dougabka, D., Edwards, D. P., Evans, R., Falster, D., Fearnside, P., Flores, O., Fyllas, N.,
711 Gérard, J., Goodman, R. C., Guibal, D., Henao-Diaz, L. F., Hervé, V., Hietz, P., Homeier, J.,
712 Ibanez, T., Ilic, J., Jansen, S., Kalita, R. M., Kenzo, T., Kindermann, L., Kothandaraman, S.,
713 Kotowska, M., Kubota, Y., Langbour, P., Lawson, J., de Lima, A. L. A., Link, R. M., Linstädter,
714 A., López, R., Macinnis-Ng, C., Magnago, L. F. S., Martin, A. R., Matheny, A. M., McCarthy,
715 J. K., Miller, R. B., Nath, A. J., Nelson, B. W., Njana, M., Nogueira, E. M., Oliveira, A.,
716 Oliveira, R., Olson, M., Onoda, Y., Paul, K., Piotto, D., Radtke, P., Razafindratsima, O.,
717 Ramananantoandro, T., Read, J., Richardson, S., de la Riva, E. G., Rodríguez-Reyes, O., Rolim,
718 S. G., Rolo, V., Rosell, J. A., Salguero-Gómez, R., Santini, N. S., Schuldt, B., Schwendenmann,
719 L., Sellin, A., Staples, T., Stevenson, P. R., Sundarapandian, S., van der Sande, M. T., Thibaut,
720 B., Tng, D. Y. P., Torezan, J. M. D., Villanueva, B., Weiskittel, A., Wells, J., Wright, S. J., and
721 Zieminska, K.: Beyond species means – the intraspecific contribution to global wood density
722 variation, New Phytologist, 249, 2630-2651, https://doi.org/10.1111/nph.70860, 2026.

723 Flores, O. and Coomes, D. A.: Estimating the wood density of species for carbon stock
724 assessments, Methods in Ecology and Evolution, 2, 214-220, 2011.

Forestry Department: Ministry of Lands Natural Resources and Environmental Protection, Integrated Land Use Assessment Phase II - Technical Paper 3, *Assessment of Existing Models for Biomass Volume Calculations*. Food and Agricultural Organization of the United Nations, Ministry of Foreign Affairs Finland. Lusaka, Zambia., 59, 2016.

Goodman, R. C., Phillips, O. L., and Baker, T. R.: The importance of crown dimensions to improve tropical tree biomass estimates, Ecological Applications, 24, 680-698, 2014.

Govaerts, R., Nic Lughadha, E., Black, N., Turner, R., and Paton, A.: The World Checklist of Vascular Plants, a continuously updated resource for exploring global plant diversity, Scientific Data, 8, 215, 10.1038/s41597-021-00997-6, 2021.

Grantham, H. S., Duncan, A., Evans, T. D., Jones, K. R., Beyer, H. L., Schuster, R., Walston, J., Ray, J. C., Robinson, J. G., Callow, M., Clements, T., Costa, H. M., DeGemmis, A., Elsen, P. R., Ervin, J., Franco, P., Goldman, E., Goetz, S., Hansen, A., Hofsvang, E., Jantz, P., Jupiter, S., Kang, A., Langhammer, P., Laurance, W. F., Lieberman, S., Linkie, M., Malhi, Y., Maxwell, S., Mendez, M., Mittermeier, R., Murray, N. J., Possingham, H., Radachowsky, J., Saatchi, S., Samper, C., Silverman, J., Shapiro, A., Strassburg, B., Stevens, T., Stokes, E., Taylor, R., Tear, T., Tizard, R., Venter, O., Visconti, P., Wang, S., and Watson, J. E. M.: Anthropogenic modification of forests means only 40% of remaining forests have high ecosystem integrity, Nature Communications, 11, 5978, 10.1038/s41467-020-19493-3, 2020.

GRZ: Zambia's Forest Reference Emissions Level Submission to the UNFCCC, 41, https://redd.unfccc.int/files/2016_submission_frel_zambia.pdf Date Accessed: 20/12/2021, 2016.

GRZ: Zambia's Forest Reference Emissions Level Submission to the UNFCCC, 41, https://redd.unfccc.int/files/zambia_frel-2020-technical_assessment.pdf Date Accessed: 20/01/2022, 2021.

Guedes, B. S., Sitoe, A. A., and Olsson, B. A.: Allometric models for managing lowland miombo woodlands of the Beira corridor in Mozambique, Global ecology and conservation, 13, e00374, 2018.

Handavu, F., Syampungani, S., Sileshi, G. W., and Chirwa, P. W.: Aboveground and belowground tree biomass and carbon stocks in the miombo woodlands of the Copperbelt in Zambia, Carbon Management, 1-15, 2021.

Henry, M., Bombelli, A., Trotta, C., Alessandrini, A., Birigazzi, L., Sola, G., Vieilledent, G., Santenoise, P., Longuetaud, F., Valentini, R., Picard, N., and Saint-André, L.: GlobAllomeTree: international platform for tree allometric equations to support volume, biomass and carbon assessment, iForest - Biogeosciences and Forestry, 6, 326-330, 10.3832/ifor0901-006, 2013.

Hijmans, R.: _terra: Spatial Data Analysis_. R package version 1.7-39,, <https://CRAN.R-project.org/package=terra>. 2023.

Hua, F., Liu, M., and Wang, Z.: Integrating forest restoration into land-use planning at large spatial scales, Current Biology, 34, R452-R472, 10.1016/j.cub.2024.02.034, 2024.

ILUA: Integrated land use assessment phase II–report for Zambia, The Food and Agriculture Organization of the United Nations and the Forestry Department, Ministry of Lands and Natural Resources, Lusaka, Zambia, www. zmb-nfms. org/iluaii/index. php, 2016.

Jucker, T., Bongalov, B., Burslem, D. F. R. P., Nilus, R., Dalponte, M., Lewis, S. L., Phillips, O. L., Qie, L., and Coomes, D. A.: Topography shapes the structure, composition and function of tropical forest landscapes, Ecology Letters, 21, 989-1000, https://doi.org/10.1111/ele.12964, 2018.

Jucker, T., Caspersen, J., Chave, J., Antin, C., Barbier, N., Bongers, F., Dalponte, M., van Ewijk, K. Y., Forrester, D. I., and Haeni, M.: Allometric equations for integrating remote sensing imagery into forest monitoring programmes, Global change biology, 23, 177-190, 2017.

Jucker, T., Gosper, C. R., Wiehl, G., Yeoh, P. B., Raisbeck-Brown, N., Fischer, F. J., Graham, J., Langley, H., Newchurch, W., O'Donnell, A. J., Page, G. F. M., Zdunic, K., and Prober, S. M.: Using multi-platform LiDAR to guide the conservation of the world's largest temperate woodland, Remote Sensing of Environment, 296, 113745, https://doi.org/10.1016/j.rse.2023.113745, 2023.

Jucker, T., Fischer, F. J., Chave, J., Coomes, D. A., Caspersen, J., Ali, A., Loubota Panzou, G. J., Feldpausch, T. R., Falster, D., Usoltsev, V. A., Adu-Bredu, S., Alves, L. F., Aminpour, M., Angoboy, I. B., Anten, N. P. R., Antin, C., Askari, Y., Muñoz, R., Ayyappan, N., Balvanera, P., Banin, L., Barbier, N., Battles, J. J., Beeckman, H., Bocko, Y. E., Bond-Lamberty, B., Bongers, F., Bowers, S., Brade, T., van Breugel, M., Chantrain, A., Chaudhary, R., Dai, J., Dalponte, M., Dimobe, K., Domec, J.-C., Doucet, J.-L., Duursma, R. A., Enríquez, M., van Ewijk, K. Y., Farfán-Rios, W., Fayolle, A., Forni, E., Forrester, D. I., Gilani, H., Godlee, J. L., Gourlet-

Fleury, S., Haeni, M., Hall, J. S., He, J.-K., Hemp, A., Hernández-Stefanoni, J. L., Higgins, S. I., Holdaway, R. J., Hussain, K., Hutley, L. B., Ichie, T., Iida, Y., Jiang, H.-s., Joshi, P. R., Kaboli, H., Larsary, M. K., Kenzo, T., Kloeppel, B. D., Kohyama, T., Kunwar, S., Kuyah, S., Kvasnica, J., Lin, S., Lines, E. R., Liu, H., Lorimer, C., Loumeto, J.-J., Malhi, Y., Marshall, P. L., Mattsson, E., Matula, R., Meave, J. A., Mensah, S., Mi, X., Momo, S., Moncrieff, G. R., Mora, F., Nissanka, S. P., O'Hara, K. L., Pearce, S., Pelissier, R., Peri, P. L., Ploton, P., Poorter, L., Pour, M. J., Pourbabaei, H., Dupuy-Rada, J. M., Ribeiro, S. C., Ryan, C., Sanaei, A., Sanger, J., Schlund, M., Sellan, G., Shenkin, A., Sonké, B., Sterck, F. J., Svátek, M., Takagi, K., Trugman, A. T., Ullah, F., Vadeboncoeur, M. A., Valipour, A., Vanderwel, M. C., Vovides, A. G., Wang, W., Wang, L.-Q., Wirth, C., Woods, M., Xiang, W., Ximenes, F. d. A., Xu, Y., Yamada, T., and Zavala, M. A.: Tallo: A global tree allometry and crown architecture database, Global Change Biology, 28, 5254-5268, https://doi.org/10.1111/gcb.16302, 2022.

Jucker, T., Fischer, F. J., Chave, J., Coomes, D. A., Caspersen, J., Ali, A., Loubota Panzou, G. J., Feldpausch, T. R., Falster, D., Usoltsev, V. A., Jackson, T. D., Adu-Bredu, S., Alves, L. F., Aminpour, M., Angoboy Ilondea, B., Anten, N. P. R., Antin, C., Askari, Y., Ayyappan, N., Banin, L. F., Barbier, N., Battles, J. J., Beeckman, H., Bocko, Y. E., Bond-Lamberty, B., Bongers, F., Bowers, S., van Breugel, M., Chantrain, A., Chaudhary, R., Dai, J., Dalponte, M., Dimobe, K., Domec, J.-C., Doucet, J.-L., Dupuy Rada, J. M., Duursma, R. A., Enríquez, M., van Ewijk, K. Y., Farfán-Rios, W., Fayolle, A., Ferretti, M., Forni, E., Forrester, D. I., Gilani, H., Godlee, J. L., Haeni, M., Hall, J. S., He, J.-K., Hemp, A., Hernández-Stefanoni, J. L., Higgins, S. I., Holdaway, R. J., Hussain, K., Hutley, L. B., Ichie, T., Iida, Y., Jiang, H.-S., Joshi, P. R., Kaboli, H., Kazempour Larsary, M., Kenzo, T., Kloeppel, B. D., Kohyama, T. S., Kunwar, S., Kuyah, S., Kvasnica, J., Lin, S., Lines, E. R., Liu, H., Lorimer, C., Loumeto, J.-J., Malhi, Y., Marshall, P. L., Mattsson, E., Matula, R., Meave, J. A., Mensah, S., Mi, X., Momo, S. T., Moncrieff, G. R., Mora, F., Muñoz, R., Nissanka, S. P., Nur Hajar, Z. S., O'Hara, K. L., Pearce, S., Pelissier, R., Peri, P. L., Ploton, P., Poorter, L., Pour, M. J., Pourbabaei, H., Ribeiro, S. C., Ryan, C., Sanaei, A., Sanger, J., Schlund, M., Sellan, G., Shenkin, A., Sonké, B., Sterck, F. J., Svátek, M., Takagi, K., Trugman, A. T., Vadeboncoeur, M. A., Valipour, A., Vanderwel, M. C., Vovides, A. G., Waldner, P., Wang, W., Wang, L.-Q., Wirth, C., Woods, M., Xiang, W., de Aquino Ximenes, F., Xu, Y., Yamada, T., Zavala, M. A., and Zimmermann, N. E.: The global spectrum of tree crown architecture, Nature Communications, 16, 4876, 10.1038/s41467-025-60262-x, 2025.

Kachamba, D., Eid, T., and Gobakken, T.: Above-and belowground biomass models for trees in the miombo woodlands of Malawi, Forests, 7, 38, 2016.

Kanja, K., Zhang, C., and Atkinson, P. M.: Evaluating multi-seasonal SAR and optical imagery for above-ground biomass estimation using the national forest inventory of Zambia, International Journal of Applied Earth Observation and Geoinformation, 139, 104494, https://doi.org/10.1016/j.jag.2025.104494, 2025.

Kapinga, K., Syampungani, S., Kasubika, R., Yambayamba, A. M., and Shamaoma, H.: Species-specific allometric models for estimation of the above-ground carbon stock in miombo woodlands of Copperbelt Province of Zambia, Forest ecology and management, 417, 184-196, 2018.

Kearsley, E., De Haulleville, T., Hufkens, K., Kidimbu, A., Toirambe, B., Baert, G., Huygens, D., Kebede, Y., Defourny, P., and Bogaert, J.: Conventional tree height–diameter relationships significantly overestimate aboveground carbon stocks in the Central Congo Basin, Nature communications, 4, 2269, 2013.

Köhl, M., Neupane, P. R., and Mundhenk, P.: REDD+ measurement, reporting and verification – A cost trap? Implications for financing REDD+MRV costs by result-based payments, Ecological Economics, 168, 106513, https://doi.org/10.1016/j.ecolecon.2019.106513, 2020.

Kuyah, S., Sileshi, G. W., and Rosenstock, T. S.: Allometric models based on bayesian frameworks give better estimates of aboveground biomass in the miombo woodlands, Forests, 7, 13, 2016.

Larjavaara, M. and Muller-Landau, H. C.: Measuring tree height: a quantitative comparison of two common field methods in a moist tropical forest, Methods in Ecology and Evolution, 4, 793-801, 2013.

Ledo, A., Cornulier, T., Illian, J. B., Iida, Y., Kassim, A. R., and Burslem, D. F.: Re-evaluation of individual diameter: height allometric models to improve biomass estimation of tropical trees, Ecological Applications, 26, 2376-2382, 2016.

Lewis, S. L., Wheeler, C. E., Mitchard, E. T., and Koch, A.: Restoring natural forests is the best way to remove atmospheric carbon, Nature, 568, 25-28, 2019.

Lutz, J. A., Furniss, T. J., Johnson, D. J., Davies, S. J., Allen, D., Alonso, A., Anderson-Teixeira, K. J., Andrade, A., Baltzer, J., and Becker, K. M.: Global importance of large-diameter trees, Global Ecology and Biogeography, 27, 849-864, 2018.

McNicol, I. M., Ryan, C. M., and Mitchard, E. T.: Carbon losses from deforestation and widespread degradation offset by extensive growth in African woodlands, Nature communications, 9, 3045, 2018.

McNicol, I. M., Ryan, C. M., and Williams, M.: How resilient are African woodlands to disturbance from shifting cultivation?, Ecological Applications, 25, 2320-2336, https://doi.org/10.1890/14-2165.1, 2015.

Melo, J., Baker, T., Nemitz, D., Quegan, S., and Ziv, G.: Satellite-based global maps are rarely used in forest reference levels submitted to the UNFCCC, Environmental Research Letters, 18, 034021, 10.1088/1748-9326/acba31, 2023.

Mitchard, E. T., Feldpausch, T. R., Brienen, R. J., Lopez-Gonzalez, G., Monteagudo, A., Baker, T. R., Lewis, S. L., Lloyd, J., Quesada, C. A., and Gloor, M.: Markedly divergent estimates of A mazon forest carbon density from ground plots and satellites, Global Ecology and Biogeography, 23, 935-946, 2014.

Molto, Q., Hérault, B., Boreux, J.-J., Daullet, M., Rousteau, A., and Rossi, V.: Predicting tree heights for biomass estimates in tropical forests–a test from French Guiana, Biogeosciences, 11, 3121-3130, 2014.

Momo Takoudjou, S., Ploton, P., Sonké, B., Hackenberg, J., Griffon, S., de Coligny, F., Kamdem, N. G., Libalah, M., Mofack, G. I., Le Moguédec, G., Pélissier, R., and Barbier, N.: Using terrestrial laser scanning data to estimate large tropical trees biomass and calibrate allometric models: A comparison with traditional destructive approach, Methods in Ecology and Evolution, 9, 905-916, https://doi.org/10.1111/2041-210X.12933, 2018.

Mugasha, W. A., Eid, T., Bollandsås, O. M., Malimbwi, R. E., Chamshama, S. A. O., Zahabu, E., and Katani, J. Z.: Allometric models for prediction of above-and belowground biomass of trees in the miombo woodlands of Tanzania, Forest Ecology and Management, 310, 87-101, 2013.

874 Munalula, F., Seifert, T., and Meincken, M.: Inter-annual growth response of three Miombo
875 tree species to climatic effects, Southern Forests: a Journal of Forest Science, 82, 135-147,
876 10.2989/20702620.2020.1814111, 2020.

877 Olson, D. M., Dinerstein, E., Wikramanayake, E. D., Burgess, N. D., Powell, G. V. N.,
878 Underwood, E. C., D'amico, J. A., Itoua, I., Strand, H. E., Morrison, J. C., Loucks, C. J., Allnutt,
879 T. F., Ricketts, T. H., Kura, Y., Lamoreux, J. F., Wettengel, W. W., Hedao, P., and Kassem, K.
880 R.: Terrestrial Ecoregions of the World: A New Map of Life on Earth: A new global map of
881 terrestrial ecoregions provides an innovative tool for conserving biodiversity, BioScience, 51,
882 933-938, 10.1641/0006-3568(2001)051[0933:Teotwa]2.0.Co;2, 2001.

883 Pelletier, J., Paquette, A., Mbindo, K., Zimba, N., Siampale, A., Chendauka, B., Siangulube,
884 F., and Roberts, J. W.: Carbon sink despite large deforestation in African tropical dry forests
885 (miombo woodlands), Environmental Research Letters, 13, 094017, 2018.

886 Phillips, O. L., Sullivan, M. J. P., Baker, T. R., Monteagudo Mendoza, A., Vargas, P. N., and
887 Vásquez, R.: Species Matter: Wood Density Influences Tropical Forest Biomass at Multiple
888 Scales, Surveys in Geophysics, 40, 913-935, 10.1007/s10712-019-09540-0, 2019.

889 Ploton, P., Barbier, N., Momo, S. T., Réjou-Méchain, M., Boyemba Bosela, F., Chuyong, G.
890 B., Dauby, G., Droissart, V., Fayolle, A., and Goodman, R. C.: Closing a gap in tropical forest
891 biomass estimation: taking crown mass variation into account in pantropical allometries,
892 Biogeosciences, 13, 1571-1585, 2016.

893 Poppenwimer, T.: WWF Spatial Regions [dataset],
894 https://doi.org/10.6084/m9.figshare.20972071.v1, 2022.

895 Quegan, S., Le Toan, T., Chave, J., Dall, J., Exbrayat, J.-F., Minh, D. H. T., Lomas, M.,
896 D'Alessandro, M. M., Paillou, P., Papathanassiou, K., Rocca, F., Saatchi, S., Scipal, K., Shugart,
897 H., Smallman, T. L., Soja, M. J., Tebaldini, S., Ulander, L., Villard, L., and Williams, M.: The
898 European Space Agency BIOMASS mission: Measuring forest above-ground biomass from
899 space, Remote Sensing of Environment, 227, 44-60, https://doi.org/10.1016/j.rse.2019.03.032,
900 2019.

901 R Core Team: _R: A Language and Environment for Statistical Computing_. R Foundation for
902 Statistical Computing, https://www.R-project.org/, 2023.

Rathgeber, C. B., Cuny, H. E., and Fonti, P.: Biological basis of tree-ring formation: a crash course, Frontiers in Plant Science, 7, 734, 2016.

Réjou-Méchain, M., Tanguy, A., Piponiot, C., Chave, J., and Hérault, B.: biomass: an r package for estimating above-ground biomass and its uncertainty in tropical forests, Methods in Ecology and Evolution, 8, 1163-1167, https://doi.org/10.1111/2041-210X.12753, 2017.

Ribeiro, N. S., Silva de Miranda, P. L., and Timberlake, J.: Biogeography and ecology of miombo woodlands, in: Miombo woodlands in a changing environment: securing the resilience and sustainability of people and woodlands, Springer, 9-53, 2020.

Ryan, C. M., Williams, M., and Grace, J.: Above-and belowground carbon stocks in a miombo woodland landscape of Mozambique, Biotropica, 43, 423-432, 2011.

Schloerke, B., Cook, D., Larmarange, J., Briatte, F., Marbach, M., Thoen, E., Elberg, A., and Crowley, J.: GGally: Extension to 'ggplot2'. R package version 2.1.2, https://CRAN.R-project.org/package=GGally, 2021.

Sileshi, G. W.: A critical review of forest biomass estimation models, common mistakes and corrective measures, Forest Ecology and Management, 329, 237-254, 2014.

Sullivan, M. J., Lewis, S. L., Hubau, W., Qie, L., Baker, T. R., Banin, L. F., Chave, J., Cuni-Sanchez, A., Feldpausch, T. R., and Lopez-Gonzalez, G.: Field methods for sampling tree height for tropical forest biomass estimation, Methods in ecology and evolution, 9, 1179-1189, 2018.

Syampungani, S., Tigabu, M., Matakala, N., Handavu, F., and Oden, P. C.: Coppicing ability of dry miombo woodland species harvested for traditional charcoal production in Zambia: a win–win strategy for sustaining rural livelihoods and recovering a woodland ecosystem, Journal of Forestry Research, 28, 549-556, 10.1007/s11676-016-0307-1, 2017.

Terryn, L., Calders, K., Meunier, F., Bauters, M., Boeckx, P., Brede, B., Burt, A., Chave, J., da Costa, A. C. L., and D'hont, B.: New tree height allometries derived from terrestrial laser scanning reveal substantial discrepancies with forest inventory methods in tropical rainforests, Global change biology, 30, e17473, 2024.

Timberlake, J., Chidumayo, E., and Sawadogo, L.: Distribution and characteristics of African dry forests and woodlands, in: The dry forests and woodlands of Africa: managing for products

and services, edited by: Chidumayo, E. N., Gumbo, Davison J., Earthscan, London - UK, 11-41, 2010.

Wang, Y., Lehtomäki, M., Liang, X., Pyörälä, J., Kukko, A., Jaakkola, A., Liu, J., Feng, Z., Chen, R., and Hyyppä, J.: Is field-measured tree height as reliable as believed–A comparison study of tree height estimates from field measurement, airborne laser scanning and terrestrial laser scanning in a boreal forest, ISPRS Journal of Photogrammetry and Remote Sensing, 147, 132-145, 2019.

White, F.: The vegetation of Africa, Unesco, Paris1983.

Wickham, H., Averick, M., Bryan, J., Chang, W., McGowan, L. D. A., François, R., Grolemund, G., Hayes, A., Henry, L., and Hester, J.: Welcome to the Tidyverse, Journal of open source software, 4, 1686, 2019.

Wilke, C.: _cowplot: Streamlined Plot Theme and Plot Annotations for 'ggplot2'_. R package version 1.1.1, <https://CRAN.R-project.org/package=cowplot>. 2020.

Williams, M., Ryan, C., Rees, R., Sambane, E., Fernando, J., and Grace, J.: Carbon sequestration and biodiversity of re-growing miombo woodlands in Mozambique, Forest Ecology and management, 254, 145-155, 2008.

Yambayamba, A. M., Fischer, F. J., and Jucker, T.: Competition, Precipitation, and Temperature Shape Deviations From Scaling Laws in the Crown Allometries of Miombo Woodlands, Biotropica, 57, e70093, https://doi.org/10.1111/btp.70093, 2025.

Zhang, J. and Qian, H.: U.Taxonstand: An R package for standardizing scientific names of plants and animals, Plant Diversity, 45, 1-5, https://doi.org/10.1016/j.pld.2022.09.001, 2023.

Zianis, D., Muukkonen, P., Mäkipää, R., and Mencuccini, M.: Biomass and stem volume equations for tree species in Europe, Silva Fennica Monographs, 4, 1-63, 2005.